May 2023 Volume 5 Issue 2
www.pmf.ni.ac.rs/chemianaissensis

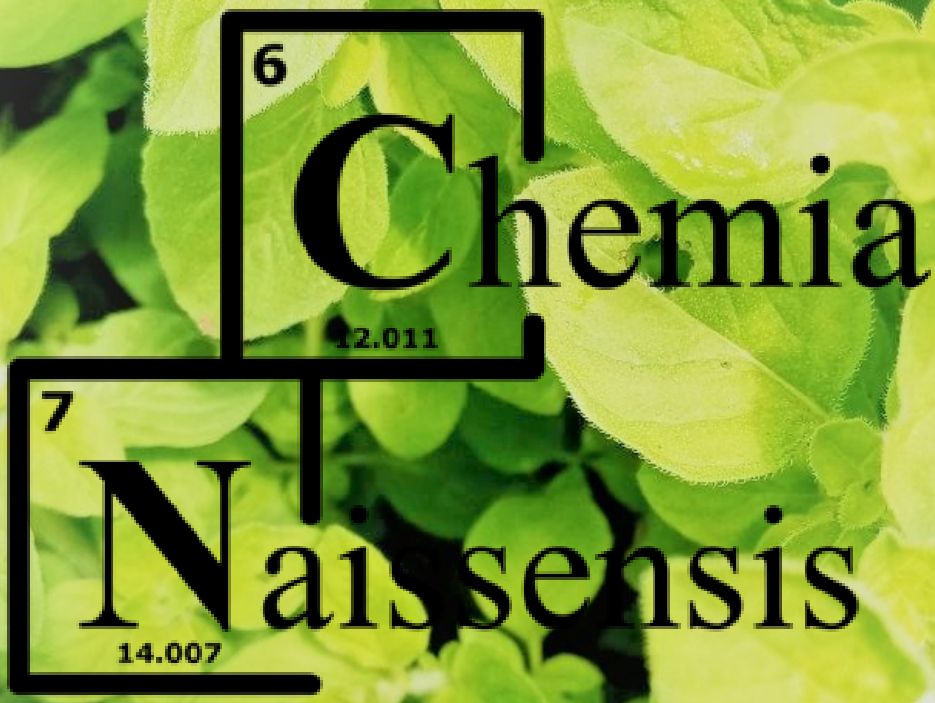

ISSN 2620-1895

University of Niš, Faculty of Sciences and Mathematics

ISSN 2620-1895

Volume 5, Issue 2

May 2023

Category: M53

https://ezproxy.nb.rs:2058/upload/documents/MNTR/Kategorizacija_casopisa/2022/MNTR2022_hemija.pdf

Publisher:

Faculty of Sciences and Mathematics, University of Niš

Chemical Engineering
Dr Marjan Ranđelović, Department of Chemistry, Faculty of Sciences and Mathematics, University of Niš, Republic of Serbia

Chemical Education
Dr Vesna Stankov Jovanović, Department of Chemistry, Faculty of Sciences and Mathematics, University of Niš, Republic of Serbia

Language Editors:

1. **Dr Selena Stanković**, Department of French Language and Literature, Faculty of Philosophy, University of Niš, Serbia (French)
2. **MA Sofija Filipović**, Department of French Language and Literature, Faculty of Philosophy, University of Niš, Serbia (French)
3. **Dr Nikoleta Momčilović**, Department of German Language, Faculty of Philosophy, University of Niš, Serbia (German)
4. **Katarina Stamenković**, Department of German Language, Faculty of Philosophy, University of Niš, Serbia (German)
5. **Dr Nadežda Jović**, Department of Serbian Language and literature, Faculty of Philosophy, University of Niš, Serbia (Serbian)
6. **Jelena Stošić**, Department of Serbian Language and literature, Faculty of Philosophy, University of Niš, Serbia (Serbian)
7. **Dr Tatjana Đekić,** Department of Geography, Faculty of Science and Mathematics, University of Niš, Serbia (Russian)

PR Manager:

Dr Radomir Ljupković, Department of Chemistry, Faculty of Sciences and Mathematics, University of Niš, Republic of Serbia

Technical Secretary:

1. **Dr Jelena Nikolić**, Department of Chemistry, Faculty of Sciences and Mathematics, University of Niš, Republic of Serbia
2. **Milica Nikolić**, Department of Chemistry, Faculty of Sciences and Mathematics, University of Niš, Republic of Serbia

IT Support:

Predrag Nikolić, Haed of the Informational&Computional Center of Faculty of Science and Mathematics, University of Niš, Republic of Serbia

Cover design:

Dr Vesna Stankov Jovanović

CONTENT

Chemia Naissensis, Vol 5, Issue 2, RESEARCH ARTICLE, 1-17 DOI: 10.46793/ChemN5.2.01Z

Nickel(II) interactions with chlorophylls in solution: impact to degradation induced by UV-irradiation

Jelena Zvezdanović[1*], Sanja Petrović[1], Aleksandar Lazarević[1]

1-University of Niš, Faculty of Technology, Bulevar Oslobodjenja 124, 16000 Leskovac, Serbia

ABSTRACT

Chlorophylls and metal substituted complexes of chlorophylls with known photosensitizing abilities can be used in many types of biological and solar energy applications; thus, it is important to analyze their basic properties when they are treated by visible light and/or UV radiation. Nickel(II) can replace central magnesium from chlorophyll (Chl) molecule to form a metal substituted, "central" Ni-Chl complex. So, the possible formation of nickel-chlorophyll complexes in 95% ethanol at 40 °C was studied by UHPLC-DAD chromatography (UltraHigh Performance Liquid Chromatography–Diode Array Detector). Nickel(II)-chlorophylls interactions in the reaction solutions at 40 °C lead not only to the formation of the Ni-related Chls, Ni-Chl complexes but several oxidation and demetalation products of chlorophylls. On the other hand, the influence of nickel(II) – chlorophyll interactions on chlorophylls solutions stability under continual UV-A, -B, and -C irradiation in 95% ethanol, was followed by UV-Vis spectrophotometry. Chlorophylls as well as their reaction solutions with nickel(II) undergo photochemical degradation obeying first-order kinetics. In general, the degradation is "energy-dependent", *i.e*. proportional to the UV photons energy input. Chlorophylls are less stable than their reaction solutions with nickel(II), probably due to the higher stability of Ni-chlorophylls complexes, to all three subranges of UV-irradiation.

Keywords: chlorophyll, nickel, complex, UV-irradiation

[*] Corresponding author: jelite74@yahoo.com

Introduction

Porphyrins and their metal derivatives have attracted significant attention in various areas because of their role in many types of biomolecules such as chlorophylls, as well as in numerous biological and solar energy applications (Ali & van Lier, 1999; Bozja et al., 2003; Er et al., 2015; Kay & Grätzel, 1993; Kay et al., 1994; Kruth et al., 2014; Youssef et al., 2018). These applications are using light or UV irradiation treatments of the porphyrins (as well as chlorophylls) and their metal derivatives leading to the excitation and triplet excited states formation in so-called photosensitizing reactions. Chlorophyll as the major photosynthetic pigment is dihydroporphyrin *i.e.*, chlorine, with four pyrrole rings coordinated with magnesium; it also contains a long hydrophobic side chain derived from phytol (Figure 1). Higher plants mostly contain chlorophyll *a* and chlorophyll *b* (Chl*a* and Chl*b*, respectively). Many heavy metals (such as copper and nickel), can easily replace labile-bonded central magnesium to form metal substituted, "central" M-Chl complexes. Detailed consequences of these reactions *in vivo* and general reactions of chlorophylls with metals *in vitro* have been already discussed (Clijsters & van Assche, 1985; Drzewiecka-Matuszek et al., 2005; Grajek et al., 2020; Küpper et al., 1996, 2002, 2006; Luna et al., 1994; Molas, 2002). Nickel is considered to be an essential micronutrient for plants (Eskew et al., 1983), but at higher concentrations, this metal becomes toxic for the majority of plant species (Gajewska et al., 2006; Küpper et al., 2006; McIlveen & Negusanti, 1994; Molas, 2002; Zehetner et al., 2002). Nickel-chlorophylls were taken into account in dye-sensitized solar cells applications (Pratiwi et al., 2018). Also, a nickel-chlorophyll derivative has been already used as a multimodal agent for tumor imaging and photodynamic therapy which uses a light treatment for that purpose (Er et al., 2015). That's why the examination of chlorophylls basic properties (porphyrins in general) and their metal-complexes when they are treated by UV light is common for numerous biological and solar energy applications. The aims of this work were to examine Ni(II) – chlorophyll interactions in a way to determine the possible formation of the corresponding metal complexes (Ni-Chl) in solutions, *in vitro*, and show how Ni(II) – chlorophyll interactions influenced chlorophylls stability against continual UV irradiation in three used subranges, UV-A, UV-B, and UV-C. The results of Ni(II) – chlorophyll interactions were studied by using UV-Vis spectrophotometry and UHPLC chromatography coupled with DAD (UltraHigh Performance Liquid Chromatography – Diode Array Detector) while the UV irradiation effects were studied by UV-Vis spectrophotometry.

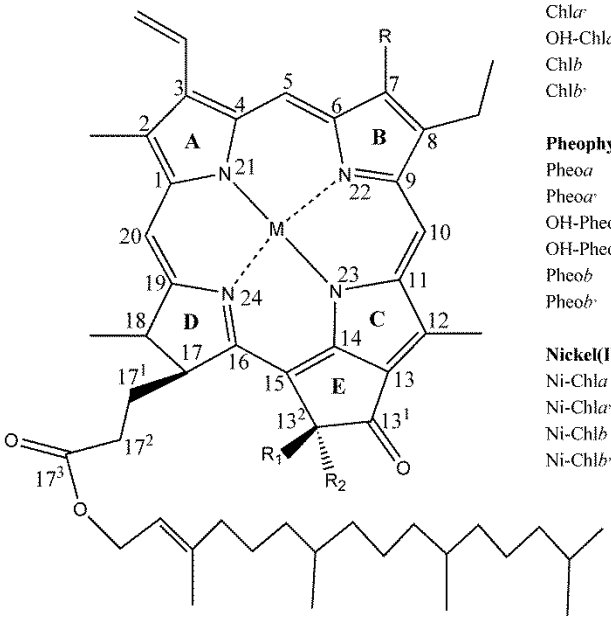

	R	R_1	R_2	M
Chlorophyll (Chl):				
Chl*a*	CH_3	H	$COOCH_3$	Mg
Chl*a'*	CH_3	$COOCH_3$	H	Mg
OH-Chl*a*	CH_3	OH	$COOCH_3$	Mg
Chl*b*	CHO	H	$COOCH_3$	Mg
Chl*b'*	CHO	$COOCH_3$	H	Mg
Pheophytin (Pheo):				
Pheo*a*	CH_3	H	$COOCH_3$	2H
Pheo*a'*	CH_3	$COOCH_3$	H	2H
OH-Pheo*a*	CH_3	OH	$COOCH_3$	2H
OH-Pheo*a'*	CH_3	$COOCH_3$	OH	2H
Pheo*b*	CHO	H	$COOCH_3$	2H
Pheo*b'*	CHO	$COOCH_3$	H	2H
Nickel(II)-chlorophyll complexes (Ni-Chl):				
Ni-Chl*a*	CH_3	H	$COOCH_3$	Ni
Ni-Chl*a'*	CH_3	$COOCH_3$	H	Ni
Ni-Chl*b*	CHO	H	$COOCH_3$	Ni
Ni-Chl*b'*	CHO	$COOCH_3$	H	Ni

Figure 1. Structures of chlorophylls discussed in this paper (Petrović et al., 2017; Zvezdanović et al. 2014).

Experimental

The solvents used in the experiments were HPLC grade. Methanol and acetonitrile used in UHPLC experiments were purchased from Baker, The Netherlands, and Fisher Scientific, UK, respectively. Ethanol and crystalline Ni(II) chloride hexahydrate were purchased from Zorka, Serbia, and Sigma–Aldrich, Germany, respectively.

The experimental procedure described below was performed under "shade" conditions as much as possible, inside vessels and equipment covered with aluminum foil to prevent photooxidation of chlorophylls (Hynninen, 1991).

Chlorophylls isolation

Chlorophylls were extracted from spinach leaves (*Spinacia oleracea* L.) using a modified method proposed by Svec (Svec, 1978, 1991; Zvezdanović et al., 2014). The obtained extract was

a mixture of pigments containing a large amount of various Chl-forms (predominantly Chl*a* and Chl*b*) as well as accessory pigments, carotenoids. The chlorophylls (*i.e.* Chl-fraction) were isolated using a modified procedure of Svec (1978) and Backman & Risch (1991), by open column chromatography with silica gel as the adsorbent and *n*-hexane/acetone mixtures as the eluent, in gradient elution regime (Zvezdanović et al., 2014). The concentration of Chl*a*, Chl*b*, and total carotenoids in 95% ethanol (*v*/*v*) was determined spectrophotometrically in the chlorophyll fraction (Lichtenthaler, 1987), showing the predominant contribution of Chl*a* (molar ratio Chl*a*:Chl*b* > 5:1) and absence of the carotenoids.

Nickel(II)-chlorophyll reaction solutions

Solid chlorophylls obtained by evaporation of solution in the stream of nitrogen were dissolved in 95% ethanol (*v*/*v*) and a solution of $NiCl_2$ was then added to adjust the final concentrations of chlorophylls and Ni(II) in the reaction solution - 2×10^{-5} mol/dm^3 and 5×10^{-5} mol/dm^3, respectively. The reaction between Chl molecules and Ni(II) in a molar ratio 1 : 2.5, was performed by heating of reaction solution on the reflux apparatus for 60 min at 40 ºC, according to the modified method proposed by Küpper (Küpper et al., 2000; Zvezdanović et al., 2012). The same experiments were done with chlorophylls in 95% ethanol (*v*/*v*) without Ni(II), as a "control sample" for 60 min of incubation.

UV-irradiation treatment

Continuous irradiation of chlorophylls, as well as Ni(II) – chlorophyll reaction solutions (after 60 min of incubation in 95% ethanol, *v*/*v*) was performed in a cylindrical photochemical reactor "Rayonnet" with eight symmetrically placed Hg-lamps having emission maxima at 350 nm (UV-A), 300 nm (UV-B) and 254 nm (UV-C). The samples were irradiated in quartz cells (1 × 1 × 4.5 cm) placed on a rotating circular holder. The total measured energy flux (hitting the samples) was 10.3 W/m^2 for 350 nm, 12.0 W/m^2 for 300 nm, and 14.3 W/m^2 for 254 nm, at 10 cm distance from the lamps. The energy flux for UV-A and UV-B irradiation was measured by using Radiometer PRO-UV35 (Probus group) and for UV-C by using Solarmeter SM 8.0 UVC (Solartech Inc.).

UV-Vis spectrophotometry

The spectrophotometric measurements were made on a Varian Cary-100 spectrophotometer. All spectra before and after irradiation were recorded from 300 to 800 nm with 1.0 bandwidth, after different irradiation time periods, t_{irr} enabling kinetics analysis in the manner earlier described in detail (Zvezdanović & Marković, 2008). Data analysis was performed by the Origin 6 software.

Ultra-high performance liquid chromatography-diode array analysis

Liquid chromatography (ultra-high performance chromatography – UHPLC) runs were realized using a Dionex Ultimate 3000 UHPLC+ system equipped with a diode array (DAD) detector. The separations were performed on a Hypersil gold C18 column (50×2.1 mm, 1.9 µm) from the same producer, at a 25 °C temperature. The mobile phase consisted of methanol and acetonitrile with a gradient program at a flow rate of 0.200 ml min^{-1} as reported previously (Petrović et al., 2017). The injection volume was 5 µL.

Absorption UV–Vis spectra were recorded on DAD with a total spectral range between 200 and 800 nm. Complexes of chlorophylls derivatives with nickel were proposed according to their UV-Vis spectra within selected peaks from the corresponding UHPLC chromatograms by comparison with the published ones with similar chlorophyll derivatives; the rest of chlorophyll derivatives were identified by comparison of the results shown in previous work in which are used the same chromatography conditions (Petrović et. al., 2017), as well as their corresponding UV-Vis spectra obtained from UHPLC-DAD signals.

Results and Discussion

Nickel(II)-chlorophyll interactions

Absorption spectra

Absorption spectra of Ni(II)–chlorophyll reaction solutions from the beginning of nickel(II)–chlorophyll interaction at 40 ºC, following increasing time periods, were shown in Figure 2A. The corresponding absorption spectra of chlorophylls (Chl-fraction), Ni(II) – chlorophyll solution and the assumed “central” Ni-Chl complex (after 60 min of incubation) have

shown in Figure 2B. The spectrum of the assumed Ni(II) complex with chlorophyll and chlorophyll derivatives is obtained by subtraction method from the spectra of Ni(II) – chlorophyll solution and the corresponding Chl-fraction. In general, chlorophylls have two major absorption regions in the visible range (400–800 nm), producing "red" (Q_y) and "blue" (Soret or *B*) band (Hoff & Amesz, 1991). The interaction of nickel with the chlorophyll in solution was followed by using the Q_y band as a sensible indicator of central metal in the chlorophyll structure (Svec, 1978). Since for the control experiments significant changes weren't observed after 60 min incubation of Chl-fraction (not shown), the changes detected in the absorption spectra of Ni(II)–chlorophyll solutions could be assigned to the Ni(II) presence and its interactions with chlorophylls in the solution. A hypochromic effect related to the Chl absorption maximum of the Q_y band (665 nm) is observed for Ni(II)–chlorophyll solutions (Figure 2A) during the period of interaction. The formation of the substitution Ni-Chl complex is usually followed by a characteristic hypsochromic ("blue") shift of the Q_y absorption band compared to Chl itself (Boucher & Katz, 1967; Helfrich & Rüdiger, 1992; Küpper et al., 1996; Pilch et al., 2013), has been observed as a shoulder at a shorter wavelength in this work (Figure 2A).

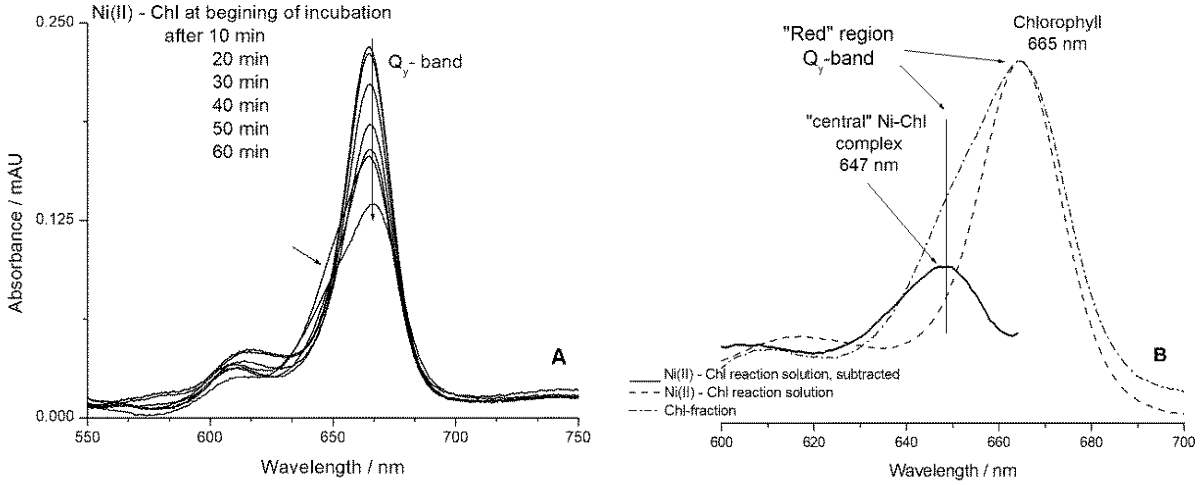

Figure 2. Absorption spectra of Ni(II)–chlorophyll reaction solutions in the "red" spectral region, following increasing periods of incubation, in 95 % ethanol (**A**). Absorption spectra of Chl in the "control" sample, Ni(II) – chlorophyll reaction solution (normalized to Q_y band absorption maximum) and assumed Ni-Chl complex, after 60 min of incubation (**B**).

This effect was clearly detected in the subtracted spectrum of Ni(II)–chlorophyll solution (Q_y band at 647 nm, Figure 2B), assumed to be for Ni-Chl complexes formed after 60 min of incubation. The term Ni-Chl complexes used in this paper refers to the substitution Ni(II) complexes of Chl*a*, Chl*b*, their conformation isomers (Chl*a*' and Chl*b*'), as well as their derivatives such as hydroxychlorophylls and potential oxidation products produced during the incubation treatment (Figure 1).

UHPLC-DAD analysis

Chromatograms of the Chl-fraction, control Chl-fraction, and Ni(II)-treated Chl-fraction (Ni(II) – chlorophyll solution), from the DAD signal at a detection wavelength, $\lambda_{det.}$ = 420 nm, were shown in Figures 3A, B, and C, respectively. The main detected Chl-derivatives with their chromatographic ($t_{ret.}$) and UV-Vis spectroscopic parameters using UHPLC-DAD data are listed in Table 1.

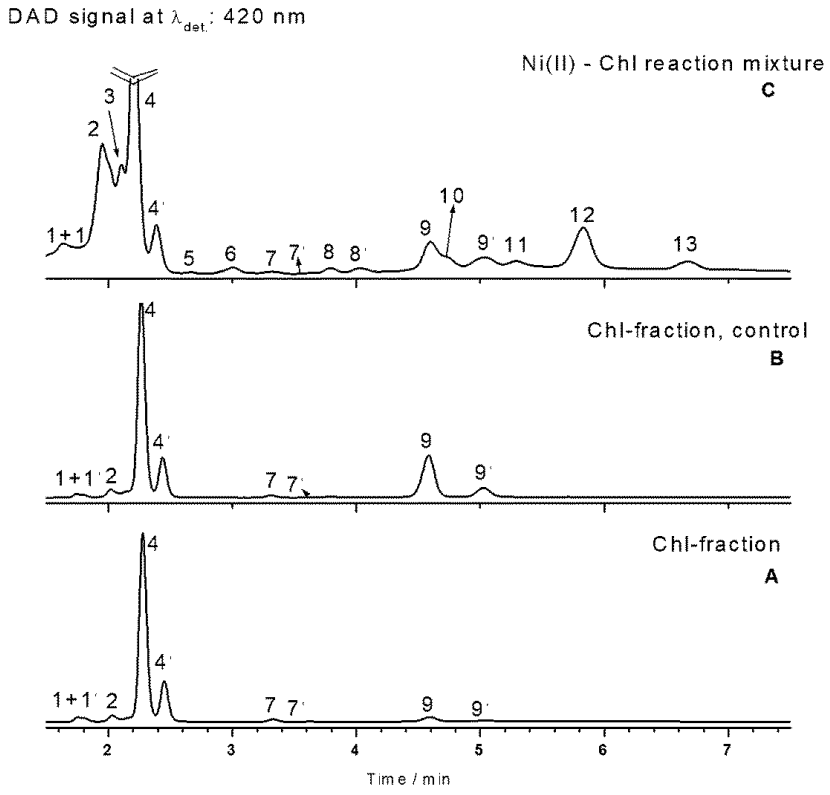

Figure 3. The UHPLC-DAD chromatograms for the Chl-fraction (**A**), "control" Chl-fraction (**B**), and Ni(II) – chlorophyll reaction solution (**C**), in 95 % ethanol after 60 min at 40 °C, recorded at 420 nm.

Chlorophyll fraction proved the presence of chlorophylls basically related to Chl*a* and Chl*b* (compounds 1, 1', 2, 7, 7', 9, 9') assigned as Chl*b*, Chl*b*', OH-Chl*a*, Pheo*b*, Pheo*b*', Pheo*a* and Pheo*a*', with the dominant contribution of Chl*a* and its conformation isomer Chl*a*' (4 and 4'), which is in accordance to UV-Vis spectrophotometric measurements; the corresponding identification was done by using previous work with the same chromatography conditions used and the corresponding absorption UV-Vis spectral data (Figure 3A, Table 1) (Petrović et al., 2017). In the control sample, incubated Chl-fraction without Ni(II) ions, no new compounds, only higher content of Pheo*a* derivatives (as a consequence of central Mg replacing by two hydrogen atoms), was detected after 60 min of incubation (comp. No. 9 and 9' in Figure 3B). In the Ni(II) – chlorophyll reaction solutions, various products, derivatives of Chls as well as Ni-Chls were detected after 60 min (Figure 3C, Table 1). Partial identification of the products was done by using absorption spectral data: Soret and Q_y bands wavelengths and absorption maximums ratios ($A_{Soret.}/A_{Qy}$) in accordance with available literature (Boucher & Katz, 1967; Pilch et al., 2013). Absorption spectra of chlorophyll *a* and its derivatives consisted of two bands, Soret at 430 nm and Q_y at 660 nm, with the corresponding absorbance ratio $A_{Soret.}/A_{Qy}$ between 1.1 and 1.3 in various solvents (Boucher & Katz, 1967; Jeffrey et al., 1996; Milenković et al., 2012); the corresponding spectra for Ni(II) complexes with Chl*a* derivatives consisted from Soret band at ≈423 nm and Q_y band at ≈652 nm, the band ratio ≈0.95 and with Chl*b* derivatives at ≈430 nm, ≈632 nm and 1.93, respectively (Boucher & Katz, 1967). Formation of Ni(II) complexes with Chl*a* and its derivatives in the Ni(II) – chlorophyll reaction solutions was assumed for compounds no. 10, 11, 12, and 13 according to the Soret band positioned at ≈420 nm, Q_y band between 644 and 654 nm (hypsochromic effect) and the absorbance maximums ratio values between 1.10 and 1.28 (Table 1) (Boucher & Katz, 1967; Pilch et al., 2013). Nickel complexes with Chl*b* or its derivatives were assumed for the compounds No. 3 and 5 according to the corresponding absorption maximums at 420 nm and 414 nm, 652 nm and 648 nm, respectively, as well as band ratio at 2.00 (Table 1) (Boucher & Katz, 1967). On the other hand, two more products in the Ni(II)-treated Chl solutions were detected, compounds no. 6 and 8 shown in Table 1. Compounds no. 8 and 8' were assigned as OH-Pheo*a* and OH-Pheo*a*', the hydroxy-pheophytins, without magnesium in the central position of chlorophyll *a* structure and OH group at C-13^2 position (Figure 1). Identification was done by considering the same chromatography conditions and spectral data from the previous

paper (Petrović et al., 2017). Compound no.6 is according to the UV-Vis spectral data certainly a chlorophyll derivative but was not fully identified (Table 1).

Table 1. Peak assignment of chlorophylls (Fig.3) separated by UHPLC-chromatography.

UHPLC-chromatography	Diode Array Detection					
Proposed structure	$t_{ret.}$/ min	Absorption maximums in the mobile phase/nm		Absorption maximums ratio	not-treated	control	Ni(II)-treated
		Soret	Q_y	$A_{Soret.}/A_{Qy}$			
1 Chl*b* 1' Chl*b*'	1.75 1.81	466	651	2.90	+	+	+
2 OH-Chl*a*	2.02	430	665	1.41	+	+	+
3 n.i. Chl*b* derivative complex with Ni	2.10	420	652	2.00	-	-	+
4 Chl*a* 4' Chl*a*'	2.27 2.44	431, 411	665	1.10	+	+	+
5 n.i. Chl*b* derivative complex with Ni	2.67	414	648	2.00	-	-	+
6 n.i. Chl derivative	3.01	427	654	7.00	-	-	+
7 Pheo*b* 7' Pheo*b*'	3.33 3.62	435	654	5.50	+	+	+
8 OH-Pheo*a* 8' OH-Pheo*a*'	3.81 4.02	407	666	2.48	-	-	+
9 Pheo*a* 9' Pheo*a*'	4.60 5.05	408	666	2.40	+	+	+
10 n.i. Chl*a* derivative complex with Ni	4.73	423, 400	652	1.10	-	-	+
11 n.i. Chl*a* derivative complex with Ni	5.28	411, 391	644	1.28	-	-	+
12 n.i. Chl*a* derivative complex with Ni	5.8	422, 401	652	1.18	-	-	+
13 n.i. Chl*a* derivative complex with Ni	6.67	422, 401	652	1.20	-	-	+

n.i. - not identified

So, Ni(II) ions and chlorophylls interactions at 40 °C in the water-ethanol reaction solutions lead not only to formation of the Ni-related Chls, but also oxidation and demetalation chlorophyll derivatives such as OH-Chl*a*, OH-Pheo*a* and their conformation isomers, as well production some

new, not identified Chl derivatives. After 60 min, full transformation of Chl*a* and its isomer Chl*a*' to the various products wasn't provided, Ni-Chl complexes formation was not the only reaction that takes place in the conditions described in this paper, at Ni : Chl molar ratio (2.5 : 1).

UV-irradiation of chlorophyll and nickel(II)-chlorophyll reaction solutions

Absorption spectra of chlorophylls (Chl-fraction) and Ni(II) – chlorophyll reaction solutions following increasing periods of continual UV-B irradiation were shown in Figures 4A and B, respectively; spectra of assumed Ni-Chl complexes obtained by subtraction method, were shown in the increment of Figure 4B. The corresponding spectra following increasing periods of continual UV-A and UV-C irradiation, have shown similar spectral behavior (not shown). The effects of UV-A, -B, and -C continuous irradiation on chlorophyll fraction and Ni(II) – chlorophyll reaction solution in 95% ethanol were followed by using UV-Vis spectrophotometric measurements; the changes were recorded at Q_y absorbance maximum values for the Chl and Ni-Chl, 665 and 647 nm, respectively.

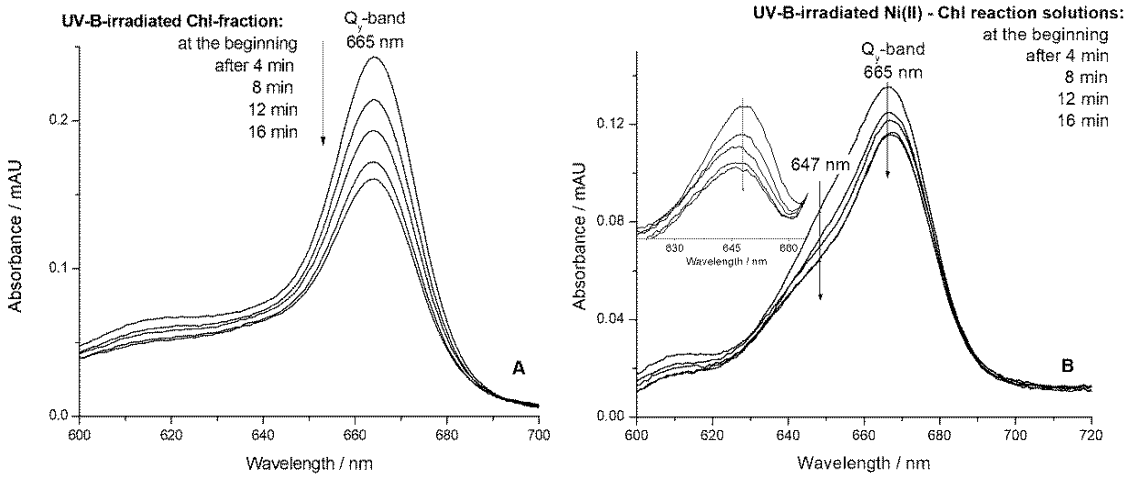

Figure 4. Continual UV-B irradiation induced degradation of chlorophyll fraction and Ni(II) – chlorophyll reaction solutions in 95% ethanol – changes in the absorption spectra during time exposure to UV-B irradiation (**A** and **B**, respectively); the corresponding spectra of assumed Ni-Chl complexes obtained by subtraction method, were shown as the increment of Figure 4B.

Continual UV irradiation of the chlorophylls and Ni(II) – chlorophyll reaction solutions induce a gradual decrease of the absorption in the whole measured spectral range (300-800 nm), *e.g.* a

hypochromic effect has been clearly observed. A gradual decrease of the Q_y-band intensity is shown in Figures 4A, and B for UV-B irradiated samples. Continual UV irradiation clearly results in the irreversible degradation – *bleaching* of chlorophylls in all samples, especially under UV-C irradiation (not shown). Similarly, UV-induced changes of chlorophylls were already detected in various solvents like acetone, *n*-hexane, and methanol-aqueous solutions (Petrović et al., 2017; Zvezdanović & Marković, 2008; Zvezdanović et al., 2009, 2012).

Chlorophylls bleaching kinetics obey a first-order law, as already reported in several papers (Petrović et al., 2017; Santabarbara, 2006; Zvezdanović & Marković, 2008; Zvezdanović et al., 2009, 2012). Nickel(II)-chlorophyll solution also obeys first-order kinetics, and all the plots show linear dependencies with the corresponding *R* values of about 0.98. Speaking about the energy input influence, UV-induced Chls bleaching rates progressively increase from UV-A to UV-C. The calculated degradation rate values of the Ni(II) – chlorophyll reaction solutions bleaching are also in proportion to the energy inputs, as expected (from UV-A to UV-C, Table 2). Calculated degradation rate constants for Chls generally show higher values than the same ones calculated from the experiments with Ni(II) – chlorophyll reaction solutions (Table 2). These differences between Chls and Ni(II) – chlorophyll reaction solutions stability against UV irradiation seem to be related to difference in the stability of Chl*a* and Ni-Chl molecules which are in major present in the samples (results of UV-Vis and UHPLC-DAD experiments). Ni(II) – chlorophyll reaction solutions are more stable compared to chlorophylls themselves, to all three subranges of UV irradiation, as shown in Table 2. For example, UV-A irradiation-induced bleaching rate constants for Ni(II) – chlorophyll reaction solution (calculated by using absorbance values at 665 nm and 647 nm) were 3.4 and 6.4 times lower, respectively, than the same calculated for chlorophyll fraction (at 665 nm, Table 2).

Generally, the stability of "central" metal complexes of chlorophylls in solutions can be explained by theoretical analysis of Falk's "stability factor" (Hynninen, 1991). The factor includes the charge number of the metal ion, the effective radius of the metal ion in Å, and Pauling's electronegativity, and its value was already used in some works (Küpper et al., 2000; Stanley et al., 1991; Zvezdanović & Marković, 2009; Zvezdanović et al., 2012). According to Falk's "stability factor", Ni-Chl complexes are more stable in comparison to the Chls themselves. Metal complexes of porphyrins (chlorophylls) which contain the metals like Ni(II) with d^8 configuration of the

corresponding energy levels have significant metal to porphyrin orbital interaction (*i.e*. metal to ligand *dπ* - backbonding), with an increased π-π* energy separation as a result, seen as a "blue" schift in the appropriate spectra (Milgrom, 1997; Petrović et al., 2006; Zvezdanović & Marković, 2008, Zvezdanović et al., 2012), as observed in presented experiments (Figure 2). So, heavy metal - nitrogen bonds in the central position of porphyrin structure seem to play a significant role in the stability of metal complexes to UV irradiation which is reflected as the corresponding higher stability of Ni(II) – chlorophyll reaction solutions (Table 2). While chlorophylls and metallochlorophylls strongly absorb in the visible range of the spectrum, they also considerably absorb in the UV spectral range used in this work (Johnson & Day, 2002). In turn, excited chlorophylls (and the corresponding Ni-Chls) can be relaxed through complex mechanisms which can lead to their degradation (bleaching). Pilch and co-workers explained the significant photostability of Ni-Chl complexes in which a symmetry of a ligand field created in the central spot of the Ni-chlorophyll molecule is very important (Pilch et al., 2013). The central N - Ni(II) bonds, formed *via* the donation of two electrons from each of the sp^2 orbitals of two central nitrogens to an empty $s-d_{x2-y2}$ hybrid centered on Ni(II), have a considerable covalent character having an effect resulting in a similarity of their equilibrium geometries in the ground and the excited states. They lead to very fast and efficient relaxation of excited Ni-Chls by conversion to molecular vibrations and dissipation as heat. The authors concluded that these Ni-substituted pigments can be a fine exemplification of symmetry control over properties of excited states of transition metal complexes (Pilch et al., 2013).

Table 2. Chlorophylls degradation kinetics by continual UV-A, UV-B, and UV-C irradiation treatments in 95% ethanol.

Irradiation treatment	Chlorophylls (at 665 nm)	Ni(II) – chlorophyll reaction solution (at 665 nm)	Ni(II) – chlorophyll reaction solution (at 647 nm)
	Rate constants, *k* / (1/min)		
UV-A	0.02605	0.00775	0.00405
UV-B	0.02638	0.01023	0.00926
UV-C	0.15063	0.04834	0.04660

Conclusion

Nickel(II)-chlorophylls interactions at 40 °C in the water-ethanol reaction solutions lead not only to the formation of the Ni-related Chls, Ni-Chl complexes (which are predominantly formed) but also several oxidation and demetalation products of chlorophylls. The time of incubation of 60 min and/or metal concentration is not enough to convert all chlorophyll content into Ni-Chl complexes. Continual UV-irradiation of the chlorophyll fraction and Ni(II) – chlorophyll solution results in irreversible bleaching obeying first-order kinetics. The bleaching rate of Chls and their Ni-complexes depends on UV-photon energy input. Nickel(II)-chlorophylls solutions are in general more stable compared to chlorophylls themselves to all three ranges of UV irradiation, due to the higher stability of the corresponding Ni-Chl complexes formed during incubation treatment. In conclusion, due to their stability, nickel complexes of chlorophylls can be the right candidates for applications that use UV light.

Acknowledgment

This work was supported by the Republic of Serbia - Ministry of Education, Science and Technological Development, Program for financing scientific research work, number 451-03-68/2022-14/200133.

Conflict-of-Interest Statement

The authors did not declare any conflict of interest.

References

Ali, H., & van Lier, J.E. (1999). Metal complexes as photo- and radiosensitizers. Chemical Reviews, 99 (9), 2379–2450.

Backman, H., & Risch, N. (1991). Preparative Chromatography. In H. Scheer (Ed.), Chlorophylls (pp. 103-114). Boca Raton: CRC Press.

Boucher, L.J., & Katz, J.J. (1967). Aggregation of metallochlorophylls. Journal of the American Chemical Society, 89 (18), 4703-4708.

Bozja, J., Sherrill, J., Michielsen, S., & Stojiljkovic I. (2003). Porphyrin-based, light-activated antimicrobial materials. Journal of Polymer Science: Part A: Polymer Chemistry, 41 (15), 2297–2303.

Clijsters, H., & van Assche, F. (1985). Inhibition of photosynthesis by heavy metals. Photosynthesis Research, 7, 31-40.

Drzewiecka-Matuszek, A., Skalna, A., Karocki, A., Stochel, G., & Fiedor, L. (2005). Effects of heavy central metal on the ground and excited states of chlorophyll. Journal of Biological Inorganic Chemistry, 10 (5), 453-462.

Er, O., Lambrecht, F.Y., Ocakoglu, K., Kayabasi, C., & Gunduz, C. (2015). Primary evaluation of a nickel-chlorophyll derivative as a multimodality agent for tumor imaging and photodynamic therapy. Journal of Radioanalytical and Nuclear Chemistry, 306, 155–163.

Eskew, D.L., Welch, R.M., & Cary, E.E. (1983). Nickel: an essential micronutrient for legumes and possibly all higher plants. Science, 222 (4624), 621–623.

Gajewska, E., Sklodovska, M., Slaba, M., & Mazur, J. (2006). Effect of nickel on antioxidative enzyme activities, proline and chlorophyll contents in wheat shoots. Biologia Plantarum, 50 (4), 653-659.

Grajek, H., Rydzyński, D., Piotrowicz-Cieślak, A., Herman, A., Maciejczyk, M., & Wieczorek, Z. (2020). Cadmium ion-chlorophyll interaction – Examination of spectral properties and structure of the cadmium-chlorophyll complex and their relevance to photosynthesis inhibition. Chemosphere, 261, 127434.

Helfrich, M., & Rüdiger, W. (1992). Various metallopheophorbides as substrates for chlorophyll synthetase. Zeitschrift für Naturforschung C, 47, 231-238.

Hoff, A.J., & Amesz, J. (1991). Visible absorption spectroscopy of chlorophylls. In H. Scheer (Ed.), Chlorophylls (pp. 723-738). Boca Raton: CRC Press.

Hynninen, P.H. (1991). Modifications. In H. Scheer (Ed.), Chlorophylls (pp. 145-209). Boca Raton: CRC Press.

Jeffrey, S.W., Mantoura, R.F.C., & Wright, S.W. (1996). Phytoplankton pigments in oceanography: guidelines to modern methods, UNESCO Publishing.

Johnson, G.A., & Day, T.A. (2002). Enhancement of photosynthesis in *Sorghum bicolor* by ultraviolet radiation. Physiologia Plantarum, 116 (4), 554–562.

Kay, A., & Grätzel, M. (1993). Artificial photosynthesis. 1. Photosensitization of TiO_2 solar cells with chlorophyll derivatives and related natural porphyrins. Journal of Physical Chemistry, 97, 6272-6277.

Kay, A., Humphry-Baker, R., & Grätzel, M. (1994). Artificial photosynthesis. 2. Investigations on the mechanism of photosensitization of nanocrystalline TiO_2 solar cells by chlorophyll derivatives. Journal of Physical Chemistry, 98, 952-959.

Kruth, A., Peglow, S., Rockstroh, N., Junge, H., Bruser, V., & Weltmann, K.-D. (2014). Enhancement of photocatalytic activity of dye sensitised anatase layers by application of a plasma-polymerized allylamine encapsulation. Journal of Photochemistry and Photobiology A: Chemistry, 290, 31–37.

Küpper, H., Küpper, F., & Spiller, M. (1996). Environmental relevance of heavy metal-substituted chlorophylls using the example of water plants. Journal of Experimental Botany, 47, 259-266.

Küpper, H., Šetlik, I., Spiller, M., Küpper, F. C., & Prášil O. (2002). Heavy metal-induced inhibition of photosynthesis: targets of in vivo heavy metal chlorophyll formation. Journal of Phycology, 38 (3), 429-441.

Küpper, H., Spiller, M., & Küpper, F.C. (2000). Photometric method for the quantification of chlorophylls and their derivatives in complex mixtures: fitting with Gauss-peak spectra. Analytical Biochemistry, 286 (2), 247-256.

Küpper, H., Küpper, F., & Spiller, M. (2006). [Heavy metal]-Chlorophylls formed in vivo during heavy metal stress and degradation products formed during digestion, extraction and storage of plant material. In B.Grimm, R.J. Porra, W. Rüdiger, H. Scheer (Eds.) Advances in Photosynthesis - Chlorophylls and Bacteriochlorophylls (pp. 67-77). Dordrecht: Kluwer Academic Publishers.

Lichtenthaler, H.K. (1987). Chlorophylls and carotenoids: pigments of photosynthetic biomembranes. Methods in Enzymology, 148, 350-382.

Luna, C.M., González, C.A., & Trippi, V.S. (1994). Oxidative damage caused by an excess of Cu in oat leaves. Plant & Cell Physiology, 35, 11-15.

McIlveen, M.D., & Negusanti, J.J. (1994). Nickel in terrestrial environment. The Science of the Total Environment, 148 (2-3), 109-138.

Milenković, S.M., Zvezdanović, J.B., Anđelković, T.D., & Marković, D.Z. (2012). The identification of chlorophyll and its derivatives in the pigment mixtures: HPLC-chromatography, visible and mass spectroscopy studies. Advanced Technologies, 1 (1), 16-24.

Milgrom, L.R. (1997). The Colours of Life: An Introduction to the Chemistry of Porphyrins and Related Compounds, Oxford: OUP.

Molas, J. (2002). Changes of chloroplast ultrastructure and total chlorophyll concentration in cabbage leaves caused by excess of organic Ni(II) complexes. Environmental and Experimental Botany, 47 (2), 115–126.

Petrović, J., Nikolić G., & Marković, D. (2006). *In vitro* complexes of copper and zinc with chlorophyll. Journal of the Serbian Chemical Society, 71 (5), 501-512.

Petrović, S., Zvezdanović, J., & Marković, D. (2017). Chlorophyll degradation in aqueous mediums induced by light and UV-B irradiation: An UHPLC-ESI-MS study. Radiation Physics and Chemistry, 141, 8-16.

Pilch, M., Dudkowiak, A., Jurzyk, B., Łukasiewicz J., Susz, A., Stochel, G., & Fiedor, L. (2013). Molecular symmetry determines the mechanism of a very efficient ultrafast excitation-to-heat conversion in Ni-substituted chlorophylls. Biochimica et Biophysica Acta (BBA)-Bioenergetics, 1827 (1), 30–37.

Pratiwi, D.D., Nurosyid, F., Kusumandari, Supriyanto, A., & Suryana, R. (2018). Effect of Ni doping into chlorophyll dye on the efficiency of dye-sensitized solar cells (DSSC). AIP Conference Proceedings, 2014, 020066. https://doi.org/10.1063/1.5054470.

Santabarbara, S. (2006). Limited sensitivity of pigment photo-oxidation in isolated thylakoids to singlet excited state quenching in photosystem II antenna. Archives of Biochemistry and Biophysics, 455 (1), 77–88.

Stanley, K.D., de la Vega, R.L., Quirke, J.M.E., Beato, B.D., & Yost R.A. (1991). Comparison of the spectroscopic properties of metalloporphyrins. Chemical Geology, 91 (2), 169- 183.

Svec, W.A. (1978). The isolation, preparation, characterization, and estimation of the chlorophylls and the bacteriochlorophylls. In D. Dolphin (Ed.) The Porphyrins (pp. 341–399). New York: Academic Press.

Svec, W.A. (1991). The distribution and extraction of the chlorophylls. In H. Scheer (Ed.), Chlorophylls (pp. 89-100). Boca Raton: CRC Press.

Youssef, Z., Colombeau, L., Yesmurzayeva, N., Baros, F., Vanderesse, R., Hamieh, T., Toufaily, J., Frochot, C., Roques-Carmes, T., & Acherar, S. (2018). Dye-sensitized nanoparticles for heterogeneous photocatalysis: Cases studies with TiO_2, ZnO, fullerene and graphene for water purification. Dyes and Pigments, 159, 49-71.

Zehetner, A., Scheer, H., Siffel, P., & Vacha, F. (2002). Photosystem II reaction center with altered pigment-composition: reconstitution of a complex containing five chlorophyll *a* per two pheophytin *a* with modified chlorophylls. Biochimica et Biophysica Acta (BBA)-Bioenergetics, 1556 (1), 21– 28.

Zvezdanović, J., & Marković, D. (2008). Bleaching of chlorophylls by UV irradiation *in vitro*: the effects on chlorophyll organization in acetone and *n*-hexane. Journal of the Serbian Chemical Society, 73 (3), 271-282.

Zvezdanović, J., & Marković, D. (2009). Copper, iron, and zinc interactions with chlorophyll in extracts of photosynthetic pigments studied by VIS spectroscopy. Russian Journal of Physical Chemistry A, 83, 1542–1546.

Zvezdanović, J., Cvetić, T., Veljović-Jovanović, S., & Marković, D. (2009). Chlorophyll bleaching by UV-irradiation *in vitro* and *in situ*: absorption and fluorescence studies. Radiation and Physics Chemistry, 78 (1), 25–32.

Zvezdanović, J.B., Petrović, S.M., Marković, D.Z., Anđelković, T.D., & Anđelković, D.H. (2014). Electrospray ionization mass spectrometry combined with ultra high performance liquid chromatography in the analysis of *in vitro* formation of chlorophyll complexes with copper and zinc. Journal of the Serbian Chemical Society, 79 (6), 689-706.

Zvezdanović, J.B., Marković, D.Z., & Milenković, S.M. (2012). Zinc(II) and copper(II) complexes with pheophytin and mesoporphyrin and their stability to UV-B irradiation: VIS spectroscopy studies. Journal of the Serbian Chemical Society, 77 (2), 187–199.

Interakcije nikla(II) sa hlorofilima u rastvoru: uticaj na degradaciju izazvanu UV zračenjem

Jelena Zvezdanović[1], Sanja Petrović[1], Aleksandar Lazarević[1]

1-Univerzitet u Nišu, Tehnološki fakultet u Leskovcu, Bulevar Oslobođenja 124, 16000 Leskovac, Srbija

SAŽETAK

Hlorofili i metalni supstituisani kompleksi hlorofila sa svojim poznatim fotosenzibiliziratorskim osobinama, mogu se koristiti u mnogim vrstama bioloških i aplikacija sa primenom solarne energije; stoga je važno analizirati njihova osnovna svojstva kada se tretiraju svetlošću i/ili UV zračenjem. Nikl(II) može da zameni centralni magnezijum iz molekula hlorofila (Chl) da bi formirao metalom supstituisani, „centralni“ Ni-Chl kompleks. Moguće formiranje kompleksa nikla sa hlorofilom u 95% etanolu na 40 °C proučavano je UHPLC-DAD hromatografijom (engl. UltraHigh Performance Liquid Chromatography-Diode Array Detector). Interakcije nikl(II)-hlorofila u reakcionim smešama na 40 °C dovode, ne samo do formiranja derivata hlorofila sa niklom, Ni-Chl kompleksa, već i nekoliko proizvoda oksidacije i demetalacije hlorofila. Sa druge strane, uticaj interakcija nikl(II)-hlorofila na stabilnost rastvora hlorofila pod dejstvom kontinuiranog UV-A, -B i -C ozračivanja u 95% etanolu, praćen je UV-Vis spektrofotometrijski. Hlorofili kao i njihovi reakcioni rastvori sa niklom(II) podležu fotohemijskoj degradaciji koja prati kinetiku prvog reda. Generalno, degradacija je „energetski zavisna“, tj. proporcionalna upadnoj energiji UV fotona. Hlorofili su manje stabilni od njihovih reakcionih smeša sa niklom(II), verovatno zbog veće stabilnosti kompleksa Ni-hlorofil, prema dejstvu sva tri podopsega UV zračenja.

Ključne reči: hlorofil, nikal, kompleks, UV-ozračivanje

Interactions du nickel(II) avec les chlorophylles en solution: impact sur la dégradation induite par le rayonnement UV

Jelena Zvezdanović[1], Sanja Petrović[1], Aleksandar Lazarević[1]

1- Université de Niš, Faculté de technologie, Bulevar Oslobodjenja 124, 16000 Leskovac, Serbie

RÉSUMÉ

Les chlorophylles et les complexes de chlorophylles substitués par des métaux ayant des capacités de photosensibilisation connues peuvent être utilisés dans de nombreux types d'applications biologiques et solaires; il est donc important d'analyser leurs propriétés de base lorsqu'ils sont traités par la lumière visible et/ou le rayonnement UV. Le nickel(II) peut remplacer le magnésium central de la molécule de chlorophylle (Chl) pour former un complexe Ni-Chl « central » substitué par un métal. Ainsi, la formation possible de complexes nickel-chlorophylle dans l'éthanol à 95% à 40°C a été étudiée par la chromatographie UHPLC-DAD (UltraHigh Performance Liquid Chromatography–Diode Array Detector). Les interactions nickel(II)-chlorophylles dans les solutions réactionnelles à 40°C conduisent non seulement à la formation des dérivés de Chls et Ni, des complexes Ni-Chl, mais aussi de plusieurs produits d'oxydation et de démétallisation des chlorophylles. D'autre part, l'influence des interactions nickel(II) – chlorophylle sur la stabilité des solutions de chlorophylle sous rayonnement UV-A, -B et -C continue dans l'éthanol à 95% a été suivie par la spectrophotométrie UV-Vis. Les chlorophylles ainsi que leurs solutions de réaction avec le nickel(II) subissent une dégradation photochimique en respectant la cinétique de premier ordre. En général, la dégradation est « dépendante de l'énergie », c'est-à-dire proportionnelle à l'énergie incidente des photons UV. Les chlorophylles sont moins stables que leurs solutions réactives avec le nickel(II), probablement en raison d'une plus grande stabilité du complexe Ni-chlorophylles, aux trois sous-gammes de rayonnement UV.

Mots-clés: chlorophylle, nickel, complexe, rayonnement UV

Взаимодействие никеля (II) с хлорофиллами в растворе: влияние на УФ-индуцированную деградацию

Елена Звезданович[1], Саня Петрович[1], Александр Лазаревич[1]

1-Нишский университет, Технологический факультет в Лесковаце, бульвар Ослободженье 124, 16000 Лесковац, Сербия

Резюме

Хлорофиллы и металлозамещенные комплексы хлорофилла с их известными фотосенсибилизирующими свойствами могут использоваться во многих типах биологических и солнечных применений, поэтому важно проанализировать их основные свойства при обработке светом и/или УФ-излучением. Никель (II) может замещать центральный магний из молекул хлорофилла (Chl) с образованием замещенного металлом „центрального“ комплекса Ni-Chl. Возможное образование комплексов никеля с хлорофиллом в 95% этаноле при 40 °C было изучено с помощью хроматографии UHPLC-DAD (англ. Ultra High Performance Liquid Chromatography - Diode Array Detector). Взаимодействие никеля (II)-хлорофилла в реакционных смесях при 40 °C приводит не только к образованию производных хлорофилла с никелем, комплексов Ni-Chl, но и к нескольким продуктам окисления и деметаллизация хлорофилла. С другой стороны, влияние взаимодействий никель - хлорофилл на стабильность растворов хлорофилла под действием непрерывного УФ-А,- В и-С облучения в 95% этаноле УФ-видимый спектрофотометрический мониторинг. Хлорофиллы, а также их реакционные растворы с никелем подвергаются фотохимической деградации, которая сопровождает кинетику первого порядка. Как правило, деградация является „энергетически зависимой“, т. е. пропорциональна энергии падения УФ-фотонов. Хлорофиллы менее стабильны, чем их реакционные смеси с никелем(II), вероятно, из-за более высокой стабильности комплекса Ni-хлорофилл, согласно действию всех трех поддиапазонов УФ-излучения.

Ключевые слова: хлорофилл, никель, комплекс, УФ-облучение

Wechselwirkungen von Nickel(II) mit Chlorophyllen in Lösung: Auswirkungen auf den Abbau durch UV-Bestrahlung

Jelena Zvezdanović[1], Sanja Petrović[1], Aleksandar Lazarević[1]

1- Universität Niš, Technische Fakultät in Leskovac, Bulevar Oslobođenja 124, 16000 Leskovac, Serbien

ABSTRAKT

Chlorophylle und metallsubstituierte Chlorophyllkomplexe mit ihren bekannten photosensibilisierenden Eigenschaften können in vielen Arten von biologischen und solarenergienutzenden Anwendungen eingesetzt werden. Daher ist es wichtig, ihre grundlegenden Eigenschaften bei Behandlung mit Licht und/oder UV-Strahlung zu analysieren.

Nickel(II) kann das zentrale Magnesium des Chlorophyllmoleküls (Chl) ersetzen und einen metallsubstituierten "zentralen" Ni-Chl-Komplex bilden. Die mögliche Bildung von Nickel-Chlorophyll-Komplexen in 95%igem Ethanol bei 40 °C wurde mittels UHPLC-DAD-Chromatographie (*UltraHigh Performance Liquid Chromatography-Diode Array Detector*) untersucht. Die Nickel(II)-Chlorophyll-Wechselwirkungen in Reaktionslösungen bei 40 °C führen nicht nur zur Bildung von Chlorophyllderivaten mit Nickel, dem Ni-Chl-Komplex, sondern auch zu mehreren Oxidations- und Demetallisierungsprodukten von Chlorophyll. Andererseits wurde der Einfluss von Nickel(II)-Chlorophyll-Interaktionen auf die Stabilität von Chlorophylllösungen unter kontinuierlicher UV-A-, UV-B- und UV-C-Bestrahlung in 95%igem Ethanol mittels UV-Vis-Spektroskopie verfolgt. Chlorophylle sowie ihre Reaktionslösungen mit Nickel(II) unterliegen einer photochemischen Degradation, die einer kinetischen Reaktion erster Ordnung folgt. Generell ist die Degradation "energieabhängig", d.h. proportional zur eintreffenden Energie der UV-Photonen. Chlorophylle sind weniger stabil als ihre Reaktionslösungen mit Nickel(II), vermutlich aufgrund der höheren Stabilität des Ni-Chlorophyll-Komplexes gegenüber der Wirkung aller drei Teilbereiche der UV-Strahlung.

Schlüsselwörter: Chlorophyll, Nickel, Komplex, UV-Bestrahlung

Midgut remodeling during the metamorphosis of *Chironomus riparius*, Meigen (1804)

Stojanović Jelena[1,2*], Savić Zdravković Dimitrija[1,2], Žabar Popović Andrea[1], Milovanović Aleksandra[2], Milošević Đurađ[1]

1-University of Niš, Faculty of Sciences and Mathematics, Department of Biology and Ecology, Višegradska 33, 18000 Niš, Serbia

2-Biological Society "Dr. Sava Petrović", Višegradska 33, 18000 Niš, Serbia

ABSTRACT

The holometabolous insects go through a complete metamorphosis that includes four life stages: egg, larva, pupa, and imago (adult). *Chironomus riparius* is a suggested model organism by the Organization for Economic Cooperation and Development (OECD) that is used in acute and chronic tests of chemicals. Tissue morphology of healthy non-biting midge larval stage was already described but the faith of the midgut digestive cells and tissue organization during the metamorphosis is unknown. We here described histological alterations of the midgut during ecdysis to distinguish them from the ones caused by toxins' negative effects. The present study showed differences in tissue architecture of the midgut in the larval, prepupal, and pupal stages of development of *C. riparius*. During ecdysis, larval digestive cells detached from the midgut epithelium and moved to the lumen. In the pupa, the larval midgut layer was replaced with an adult midgut that had considerably reduced width. These changes in the midgut tissue morphology and organization probably follow changes in the environment and feeding behavior of *C. riparius* at different stages of development.

Keywords: Chironomidae, metamorphosis, midgut, histology, xenobiotics

[*] Corresponding author: jelena.conic@pmf.edu.rs

Introduction

One of the main characteristics of holometabolous insects is their ability to go through the process of metamorphosis with an intercalated pupal stage between larva and adult. During that phase, the tissues are extensively remodeled while some of them are completely degraded (Rolff et al., 2019). Each of the phases is adapted to the specific roles in the life cycle of the organism (Hall & Martín-Vega, 2019). The family of Chironomidae (Diptera) are widely spread organisms that can adapt to diverse water ecosystems (Hilsenhoff, 2001). The aquatic model organism, suggested by the Organization for Economic Cooperation and Development (OECD) for ecotoxicological testing of chemicals is *Chironomus riparius*, Meigen, 1804 (Diptera, Chironomidae) (OECD, 2004a, b). The larvae of *C. riparius* are aquatic and active with nonselective feeding behavior. They go through 4 larval instars, which are benthic, before entering the prepupal and pupal stadium. Adults are released by eclosion from the pupa. The complete life cycle of *C. riparius* in laboratory conditions (at 20 °C) is completed in 20-28 days (Armitage et al., 1995). During the metamorphosis of chironomids as holometabolous insects, the midgut undergoes remodeling through the proliferation and differentiation of imaginal stem cells and the removal of larval midgut cells (Wu et al., 2006). Generally, the insect alimentary canal is divided into 3 regions: foregut, midgut, and hindgut (Chapman, 2012). A previous study by Stojanović et al. (2021) described the internal morphology of the *C. riparius* larvae digestive system based on histology analyses. Foregut starts with the mouth and ends in the metathorax on the place where the stomodeal valve separates the fore- and midgut. Based on digestive cell morphology, the midgut is divided into 3 regions. The transition between the midgut and hindgut is a place where the Malpighian tubules insert. Hindgut is formed by the ileum, colon, and rectum. There is a lack of information about what happens with the midgut after the metamorphosis of *C. riparius* larvae.

The industrial era has brought novel emerging contaminants to the environment that raised a concern about their ecotoxicity. Emerging contaminants were defined by the United States Environmental Protection Agency (EPA) as chemicals or materials that are a potential or real threat to human health or the environment (United States Environmental Protection Agency, 2011). Because of their extensive production and use, metal-oxide nanomaterials and microplastics have gained global attention as emerging contaminants (Maddela et al., 2022). Xenobiotics that reach waters may be deposited in sediment so detection of their presence and toxic activity is of great

importance (Gonçalves et al., 2012). For this purpose, benthic organisms are extensively used as bioindicators of toxic pollution of the sediment (Richardi et al., 2015). Even though chironomids were ecologically classified by functional feeding groups, the certain flexibility in their feeding behavior has led to the conclusion that they are opportunistic omnivores (Armitage et al., 1995). This way, they ingest xenobiotics along with the food and sediment. It was noticed in a previous study that exposure to the TiO_2 nanoparticles induced changes in the midgut similar to those described in healthy *Drosophila melanogaster* during the prepupal stage of the normal life cycle (Nelliot et al., 2006; Stojanovic et al., 2021). Nanoparticles have the potential to penetrate cells of the midgut, as shown in a study with *Ceriodaphnia dubia* (Dalai et al., 2013). The toxic potential of nanoparticles depends on their characteristics such as size, surface chemistry, and concentration (Yao et al., 2015). The general mechanism that was proposed to be the cause of nanoparticle cytotoxicity is the generation of reactive oxygen species (ROS) that could damage cells. It was described that nanoparticles have the potential to generate electrons that could enter the cells and disrupt the respiratory chain, leading to ROS overexpression and finally cell apoptosis, necrosis, and mutagenesis (Yu et al., 2020). Additionally, the insect larvae can regenerate digestive cells when exposed to xenobiotics, which cause changes in the midgut region (Castagnola & Jurat-Fuentes, 2016; Stojanovic et al., 2021). Given that apoptosis also takes a part, as one of the main processes, in midgut remodeling, it is important to distinguish the cause of the cell death by describing tissue alterations in both cases: cytotoxicity and metamorphosis (Franzetti et al., 2012).

Toxicokinetics describes processes that include absorption, distribution, metabolism, and excretion of toxins which determine the potential of the organism to handle the chemical. Toxicodynamics quantitatively describes the effect that toxin has on biological systems (Arena, 1976). The toxicodynamics and toxicokinetics of xenobiotics in *C. riparius* couldn't be understood without a description of the changes that occur during the life cycle of the healthy organism.

This study aims to describe potential changes in the morphology of the digestive system during the ecdysis of *C. riparius* larvae using histology. By defining them, we could detangle the tissue alterations caused by the direct toxic influence of xenobiotics versus indirect ones that induce ecdysis.

Experimental

Model organism

In this study, *C. riparius* Meigen, 1804, obtained from the stock culture housed at the laboratory of the Department of Biology and Ecology, Faculty of Sciences and Mathematics, University of Nis, was used. The culture is formed and maintained following OECD guidelines (OECD, 2004a). The population is cultured in glass tanks filled with a mixture of distilled and tap water (1:1) and cellulose sediment. The temperature was adjusted to 23˚C±2˚C, with a 16/8 h photoperiod and constant aeration.

Experimental setup

To detangle histological changes of the midgut during metamorphosis from the ones induced by toxins, the population of *C. riparius* larvae from one egg mass was used. The experiment was conducted in laboratory conditions at the Department of Biology and Ecology, Faculty of Sciences and Mathematics, University of Nis. A 700ml glass jar was filled with 105 cm^3 of coarse quartz sediment and poured over with a mix of distilled and tap water (50:50). The heater was placed and set to maintain the constant temperature of 23 °C ±2 °C. A 16/8h photoperiod was provided and the setup was left for 24h to stabilize the environment. The egg mass was transferred into the jar and fed regularly until the ecdysis started. After the larvae reached the 4^{th} instar, the collection of the individuals started. 10 individuals were collected each day until the emergence started. The collected 4^{th} instar larvae, prepupa, and pupa individuals were fixed in 70% alcohol and saved for further analyses.

Histology analyses

After fixation, they were dehydrated by increasing the series of alcohol (70%, 80%, 90%, and 96%) and then transferred to toluene for 10 min. The samples were placed in tissue-embedding paraffin and left overnight. The day after, samples were subjected to embedding and sectioning. Five-µm longitudinal sections, made on a Leica® RM 2125RT microtome, were stained using the combination of hematoxylin and eosin (H&E), then analyzed and photographed using Leica® DM 2500 light photomicroscope.

Results and Discussion

Out of total of 50 analysed individuals, 10 were 4th instar larvae, 22 were in the prepupal phase and 18 were in the pupal phase of development. By examining histological slides of the fourth instar larvae, all previously described elements of the midgut were detected (Stojanović et al., 2021). Morphological analyses of prepupa and pupa revealed changes in the tissue architecture of the alimentary canal during the process of ecdysis. The second layer of digestive cells was noticed in midgut region I of the prepupal stage when compared to the midgut region I of the 4th instar larvae (Figure 1A, D).

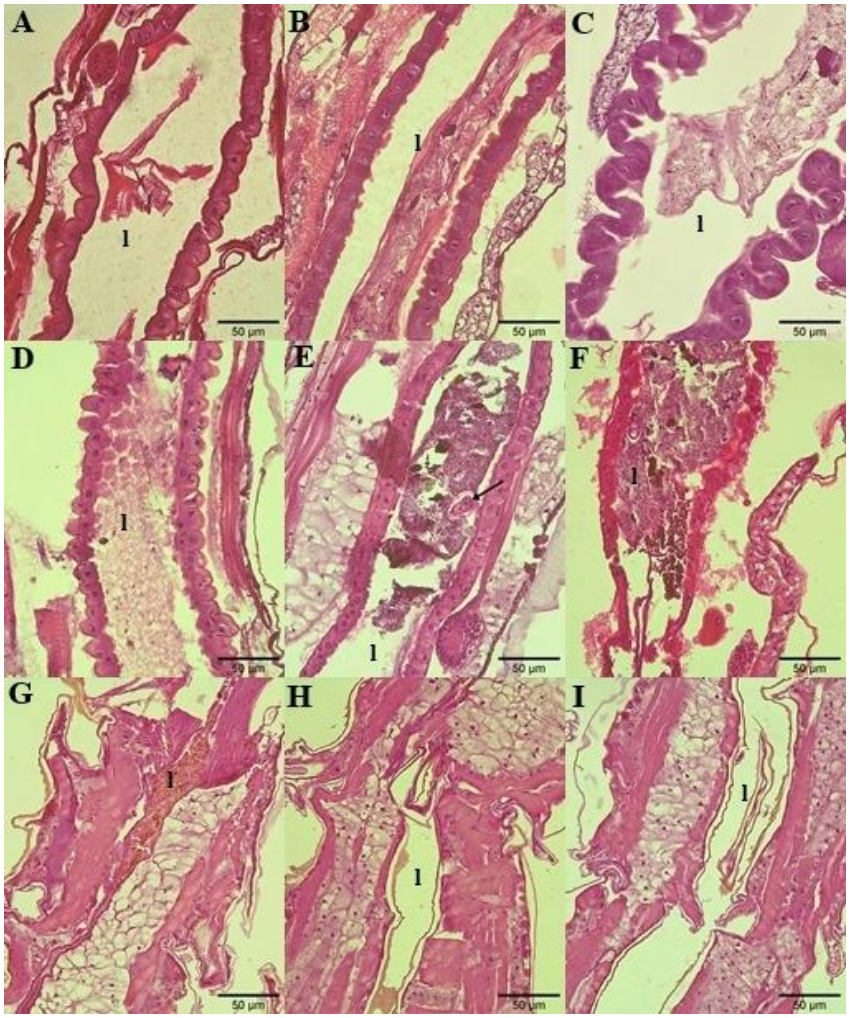

Figure 1. Photomicrographs of *C. riparius* midgut in different developmental stages. **A-C**, midgut regions I, II and III, respectivelly of the 4th larval instar; **D-F**, midgut regions I, II and III, respectively of the prepupal stage; **G-I**, midgut regions I, II and III, respectively of the pupa. Arrow (**E**) shows coated pair of cells projecting to the lumen (**l**).

In region II of the prepupal stage pair of coated cells, detached from the epithelial layer and projected to the lumen of the intestine was detected (Figure 1E). Prepupal midgut region III lost invaginations of the epithelial layer that was apparent in the larval stage (Figure 1C, F).

The midgut of the pupa showed different morphology of digestive cells in all three regions (Figure 1G, H, I). The epithelial layer was noticeably thinner and cells lost their shape that was characteristic for each midgut region (Stojanović et al., 2021). The intestinal lumen of the pupa was narrow and clear when compared to the lumen in earlier stages of development, larvae, and prepupa.

The process of metamorphosis includes certain rearrangements of the midgut of *C. riparius* (Wu et al., 2006). Richardi et al. (2018) described the midgut as one of the most sensitive tissues to the presence of toxins. To distinguish changes in the architecture of the midgut caused by ecdysis from the ones caused by toxins, a description of midgut remodeling during metamorphosis is necessary. Previous studies done on mosquitoes showed that during the prepupal stage, larval digestive cells detach from the pupal digestive cells and move to the midgut lumen completely 12h after ecdysis to the pupal stage. Eventually, pupal midgut cells differentiate and form an adult midgut with considerably reduced width (Wu et al., 2006). This strongly correlates with our study, where a detachment of the midgut cells was observed in midgut region II of the prepupal stage. The study on *Heliothis virescens* described midgut remodeling as a result of two overlapping processes which include degrading the old epithelium and generation of a new one. In the larval stage, the need for intake and accumulation of nutrients is increased so the midgut cells are metabolically active with a well-developed brush border. During the ecdysis, regenerative stem cells take the lead role and replace the larval midgut with the adult midgut (Tettamanti et al., 2007). Cell proliferation was noticed in the present study as well, where the second layer of digestive cells appeared in midgut region I. It was believed that adults of Chironomidae are not feeding because of their non-functional mouthparts, but few studies have shown that they indeed feed on sucrose (Burtt et al., 1986; Foucault et al., 2018). As it was visible on histological sections of the pupa, the lumen was more narrow and empty in midgut regions II and III, while in region I some intestinal content was detectable but distinct from the one in previous stages of development.

Conclusion

The importance of describing the changes that happen during the ecdysis lies in using histopathology as a method for ecotoxicological assessment, where normal remodeling of the midgut could easily be misunderstood as a change caused by toxin exposure (Stojanović et al., 2021). The present study showed that remodeling of the midgut does occur during the metamorphosis of the *C. riparius* where stem cells proliferated and provided new, pupal digestive cells that replaced the larval intestinal epithelium. While the new layer of digestive cells was generated, the larval digestive cells detached from the midgut and moved to the intestinal lumen. As a result, the newly formed epithelial layer of the midgut was thinner with a more narrow intestinal lumen without any visible content in regions II and III. The change of the environment and feeding behavior during different stages of development of *C. riparius* probably demands different organization of the alimentary canal that could satisfy its adult stage requirements.

Acknowledgment

This study was supported by the Serbian Ministry of Education, Science and Technological Development, Grant 451-03-47/2023-01/ 200124.

Conflict-of-Interest Statement

The authors did not declare any conflict of interest.

Informed consent

Informed consent was obtained from all individual participants included in the study.

References

Arena, J. M. (1976). Introduction to general toxicology. JAMA, 236 (19), 2226.

Armitage, P. D., Cranston, P. S., & Pinder L. C. V. (1995). The Chironomidae: Biology and ecology of non-biting midges. (1st ed.). Springer Dordrecht.

Burtt, E. T., Perry, R. J. O., & McLachlan, A. J. (1986). Feeding and sexual dimorphism in adult midges (Diptera: Chironomidae). Holartic Ecology, 9 (1), 27-32.

Castagnola, A., & Jurat-Fuentes, J. L. (2016). Intestinal regeneration as an insect resistance mechanism to entomopathogenic bacteria. Current Opinion in Insect Science, 15, 104-110.

Chapman, R. F. (2012). The Insects: Structure and Function. (4th ed.). Cambridge University Press.

Dalai, S., Pakrashi, S., Chandrasekaran, N., & Mukherjee, A. (2013). Acute toxicity of TiO_2 nanoparticles to *Ceriodaphnia dubia* under visible light and dark conditions in a freshwater system. PLoS One, 8(4), e62970.

Foucault, Q., Wieser, A., Waldvogel, A.-M., & Pfenninger, M. (2018). Establishing laboratory cultures and performing ecological and evolutionary experiments with the emerging model species *Chironomus riparius*. Journal of Applied Entomology, 143 (5), 584-592.

Franzetti, E., Huang, Z.-J., Shi, Y.-X., Xie, K., Deng, X. -J., Li, J.-P., Li, Q.-R., Yang, W.-Y., Zeng, W.-N., Casartelli, M., Deng, H.-M., Cappellozza, S., Grimaldi, A., Xia, Q., Tettamanti, G., Cao, Y., & Feng, Q. (2012). Autophagy precedes apoptosis during the remodeling of silkworm larval midgut. Apoptosis, 17(3), 305-324.

Gonçalves, S. P., Lucheta, F., de Souza, V. K., & Terra, N. R. (2012). The influence of xenobiotics in river sediment on the reproduction and survival of *Daphnia magna*, 1820, Straus. Acta Limnologica Brasiliensia, 24 (2), 220-234.

Hall, M. J. R., & Martín-Vega, D. (2019). Visualization of insect metamorphosis. Philosophical Transactions: Biological Sciences, 374 (1783), 20190071.

Hilsenhoff, W. L. (2001). Diversity and classification of insects and collembola. In J. H. Thorp & A. P. Covich (Ed.), Ecology and Classification of North American Freshwater Invertebrates (2nd ed) (pp. 661-731). Amsterdam: Elsevier.

Maddela, N. R., Ramakrishnan, B., Kakarla, D., Venkateswarlue, K., & Megharaj, M. (2022). Major contaminants of emerging concern in soils: a perspective on potential health risks. RSC Advances, 12 (20), 12396–12415.

Nelliot, A., Bond, N., & Hoshizaki, D. K. (2006). Fat-body remodeling in *Drosophila melanogaster*. Genesis, 44 (8), 396-400.

OECD (2004a) Test No. 218: Sediment-Water Chironomid Toxicity Using Spiked Sediment, OECD Guidelines for the Testing of Chemicals, Section 2, OECD Publishing, Paris.

OECD (2004b) Test No. 219: Sediment-Water Chironomid Toxicity Using Spiked Water, OECD Guidelines for the Testing of Chemicals, Section 2, OECD Publishing, Paris.

Richardi, V. S., Vicentini, M., Morais, G. S., Rebechi, D., da Silva, T. A., Fávaro, L. F. & Navarro-Silva, M. A. (2018). Effects of phenanthrene on different levels of biological organization in larvae of the sediment-dwelling invertebrate *Chironomus sancticaroli* (Diptera: Chironomidae). Environmental Pollution, 242 (A), 277-287.

Richardi, V. S., Vicentini, M., Rebechi, D., Favaro, L. F., & Navarro-Silva, M. A. (2015). Morpho-histological characterization of immature of the bioindicator midge *Chironomus sancticaroli* Strixino and Strixino (Diptera, Chironomidae). Revista Brasileira de Entomologia, 59 (3), 240-250.

Rolff, J., Johnston, P. R., & Reynolds, S. (2019). Complete metamorphosis of insects. Philosophical Transactions of the Royal Society B: Biological Sciences, 374 (1783), 20190063.

Stojanović, J. S., Milošević, Đ. D., Vitorović J. S., Savić Zdravković, D. N., Stanković, N. R., Stanković, J. B., & Vasiljević, P. J. (2021). Histopathology of *Chironomus riparius* (Diptera, Chironomidae) exposed to metal oxide nanoparticles. Archives of Biological Sciences, 73 (3), 319-329.

Tettamanti, G., Grimaldi, A., Casartelli, M., Ambrosetti, E., Ponti, B., Congiu, T., Ferrarese, R., Rivas-Pena, M. L., Pennacchio, F., & de Eguileor, M. (2007). Programmed cell death and stem cell differentiation are responsible for midgut replacement in *Heliothis virescens* during prepupal instar. Cell and Tissue Research, 330, 345–359.

United States Environmental Protection Agency. (2011). Emerging Contaminant Issues, Including Management of Emerging Contaminants in Wastewater. Emerging Contaminant Issues, Including Management Of Emerging Contaminants In Wastewater | Science Inventory | US EPA (last visited on 3.3.2023.)

Wu, Y., Parthasarathy, R., Bai, H., & Palli, S. R. (2006). Mechanisms of midgut remodeling: Juvenile hormone analog methoprene blocks midgut metamorphosis by modulating ecdysone action. Mechanisms of Development, 123 (7), 530-547.

Yao, M., He, L., McClements, D. J., & Xiao, H. (2015). Uptake of gold nanoparticles by intestinal epithelial cells: impact of particle size on their absorption, accumulation, and toxicity. Journal of Agricultural and Food Chemistry, 63 (36), 8044-8049.

Yu, Z., Li, Q., Wang, J., Yu, Y., Wang, Y., Zhou, Q., & Li, P. (2020). Reactive oxygen species-related nanoparticle toxicity in the biomedical field. Nanoscale Research Letters, 15, 115.

Remodelovanje srednjeg creva u toku metamorfoze *Chironomus riparius*, Meigen (1804)

Stojanović Jelena[1,2], Savić Zdravković Dimitrija[1,2], Žabar Popović Andrea[1], Milovanović Aleksandra[2], Milošević Đurađ[1]

1-Univerzitet u Nišu, Prirodno-matematički fakultet, Departman za biologiju i ekologiju, Višegradska 33, 18000 Niš, Srbija

2-Biološko društvo "Dr. Sava Petrović", Višegradska 33, 18000 Niš, Srbija

SAŽETAK

Holometabolni insekti podležu kompletnoj metamorfozi koja uključuje 4 razvojna stupnja: jaje, larva, lutka i imago (adult). *Chironomus riparius* je predložen model organizam od strane Organizacije za Ekonomsku Saradnju i Razvoj (OECD) koji se koristi u akutnim i hroničnim testovima ekotoksičnosti hemikalija. Morfologija tkiva zdravih larvi hironomida je već opisana, ali sudbina digestivnih ćelija srednjeg creva i organizacije tkiva u toku metamorfoze ostala je nepoznata. Kako bi pravilno razlikovali promene u srednjem crevu izazvane metamorfozom od onih izazvanih negativnim efektom toksina, neophodan je histološki opis remodelacije srednjeg creva u toku ulutkavanja. Ova studija je prva koja je opisala arhitekturu tkiva srednjeg creva u larvenom stupnju, stadijumu prepupe i stadijumu lutke kod vrste *C. riparius*. Tokom ulutkavanja, digestivne ćelije larve su se odvojile od epitela srednjeg creva i prešle u lumen. Kod lutke, larveno srednje crevo zamenjeno je adultnim koje je imalo značajno smanjenu širinu. Ove promene u morfologiji i organizaciji tkiva srednjeg creva verovatno prate promene životne sredine i načina ishrane različitih razvojnih stadijuma vrste *C. riparius*.

Ključne reči: Chironomidae, metamorfoza, srednje crevo, histologija, ksenobiotici

Remodelage de l'intestin moyen au cours de la métamorphose de *Chironomus riparius*, Meigen (1804)

Stojanović Jelena[1,2], Savić Zdravković Dimitrija[1,2], Žabar Popović Andrea[1], Milovanović Aleksandra[2], Milošević Đurađ[1]

1-Université de Niš, Faculté des sciences naturelles et des mathématiques, Département de biologie et d'écologie, Višegradska 33, 18000 Niš, Serbie

2-Société de biologie « Dr. Sava Petrović », Višegradska 33, 18000 Niš, Serbie

RÉSUMÉ

Les insectes holométaboles passent par une métamorphose complète qui comprend quatre stades de vie: œuf, larve, nymphe et imago (adulte). *Chironomus riparius* est un organisme modèle suggéré par l'Organisation de coopération et de développement économiques (OCDE) qui est utilisé dans les tests aigus et chroniques de produits chimiques. La morphologie tissulaire du stade larvaire sain de chironomidés a déjà été décrite, mais le destin des cellules digestives de l'intestin moyen et de l'organisation des tissus au cours de la métamorphose est inconnu. Pour bien distinguer les changements dans l'intestin moyen causés par la métamorphose de ceux causés par l'effet négatif des toxines, une description histologique du remodelage de l'intestin moyen lors de la pupaison est nécessaire. Cette étude est la première à décrire l'architecture tissulaire de l'intestin moyen aux stades larvaire, prénymphal et nymphal du développement de *C. riparius*. Au cours de la pupaison, les cellules digestives larvaires se sont détachées de l'épithélium de l'intestin moyen et elles se sont déplacées vers la lumière. Dans la nymphe, la couche larvaire de l'intestin moyen a été remplacée par un intestin moyen adulte dont la largeur était considérablement réduite. Ces changements dans la morphologie et l'organisation des tissus de l'intestin moyen suivent probablement des changements dans l'environnement et le comportement alimentaire de *C. riparius* à différents stades de son développement.

Mots-clés: Chironomidae, métamorphose, intestin moyen, histologie, xénobiotiques

Реконструирование средней кишки в ходе метаморфоза *Chironomus riparius*, Мейген (1804)

Стоянович Елена[1,2], Савич Здравкович Димитрия[1,2], Жабар Попович Андреа[1], Милованович Александра[2], Милошевич Джурадж[2]

1-Нишский университет, Естественно-математический факультет, кафедра биологии и экологии, Вышеградска 33, 18000 Ниш, Сербия

2-Биологическое общество "доктор. Сава Петрович", Вышеградска 33, 18000 Ниш, Сербия

Резюме

Голометаболические насекомые претерпевают полную метаморфозу, включающую 4 стадии развития: яйцо, личинка, куколка и имаго (взрослое). *Chironomus riparius* - это модельный организм предлагаемый Организацией экономического сотрудничества и развития (OECD) для оценки острой и хронической экотоксичности химических веществ. Морфология тканей здоровых личинок хирономид уже описана, но судьба пищеварительных клеток средней кишки и организации тканей в ходе метаморфоза неизвестна. Чтобы правильно отличить изменения в средней кишке, вызванные метаморфозом, от изменений, вызванных негативным эффектом токсина, необходимо гистологическое описание ремоделирования средней кишки в ходе превращения личинки в куколку. Это исследование является первым, которое описало строение ткани средней кишки на личиночной стадии, стадии препупы и стадии куколки у вида *Chironomus riparius*. На стадии куколки пищеварительные клетки личинок отделились от эпителия средней кишки и перешли в просвет. У куколки личиночная средняя кишка была заменена взрослой, которая имела значительно уменьшенную ширину. Эти изменения в морфологии и организации тканей средней кишки, вероятно, связаны с изменениями в окружающей среде и рационе питания на различных стадиях развития вида *C. riparius*.

Ключевые слова: Chironomidae, *метаморфоза, кишечник, гистология, ксенобиотики*

Umbau des Mitteldarms während der Metamorphose von *Chironomus riparius*, Meigen (1804)

Stojanović Jelena[1,2], Savić Zdravković Dimitrija[1,2], Žabar Popović Andrea[1], Milovanović Aleksandra[2], Milošević Đurađ[1]

1-Universität Niš, Mathematisch-Naturwissenschaftliche Fakultät, Abteilung für Biologie und Ökologie, Višegradska 33, 1800 Niš, Serbien

2-Biologische Gesellschaft "Dr. Sava Petrović", Višegradska 33, 18000 Niš, Serbien

ABSTRAKT

Holometabole Insekten durchlaufen eine vollständige Metamorphose, die vier Entwicklungsstadien umfasst: Ei, Larve, Puppe und Imago (adult*). Chironomus riparius* wurde von der Organisation für wirtschaftliche Zusammenarbeit und Entwicklung (OECD) als Modellorganismus für akute und chronische ökotoxikologische Tests mit Chemikalien vorgeschlagen. Die Gewebemorphologie gesunder Chironomidenlarven wurde bereits beschrieben, aber das Schicksal der Verdauungszellen des Mitteldarms und die Gewebsorganisation während der Metamorphose sind unbekannt. Um die Veränderungen im Mitteldarm, die durch die Metamorphose oder die negativen Auswirkungen von Toxinen verursacht werden, richtig zu unterscheiden, ist eine histologische Beschreibung der Umgestaltung des Mitteldarms während der Verpuppung erforderlich. Die vorliegende Studie ist die erste, die die Gewebsarchitektur des Mitteldarms im Larvenstadium, im Puppenstadium und im Larvenstadium bei der *Art C. riparius* beschrieben hat. Während der Verpuppung lösten sich die Verdauungszellen der Larve vom Epithel des Mitteldarms und traten in das Lumen ein. Bei der Puppe wurde der Mitteldarm der Larve durch den adulten Mitteldarm ersetzt, der signifikant schmaler war. Diese Veränderungen in der Morphologie und Gewebsorganisation des Mitteldarms begleiten wahrscheinlich Veränderungen in der Umwelt und Ernährungsweise der verschiedenen Entwicklungsstadien von *C. riparius*.

Schlüsselwörter: Chironomidae, Metamorphose, Mitteldarm, Histologie, Xenobiotika

Total phenolic content, antioxidant capacity, and antimicrobial activity of *Origanum heracleoticum* L., extracted with different solvents

Jovana D. Ickovski[1*], Ivan R. Palić[1], Aleksandra S. Đorđević[1], Vesna P. Stankov Jovanović[1], Violeta D. Mitić[1], Gordana S. Stojanović[1]

1- University of Niš, Faculty of Sciences and Mathematics, Department of Chemistry, Višegradska 33, 18000 Niš, Serbia

ABSTRACT

This research was based on the examination of the total phenolic content, antioxidant and antimicrobial activities of hexane, diethyl ether, ethyl acetate, and methanol extracts of *Origanum heracleoticum* L. grown in Serbia. The antimicrobial activity was determined against five bacteria and two fungi using the disk diffusion method. The total phenolic content of *O. heracleoticum* solvent extracts was determined and five different tests were used for screening of the antioxidant capacity. The highest total phenolic content was found in ethyl acetate extract (848.48 μg GAE/mg dry extract) and methanol extract (733.43 μg GAE/mg dry extract). The examination of antioxidant activity showed that methanol and ethyl acetate extracts had the strongest activity. The highest correlation was found between DPPH and FRAP (R^2 = 0.99), as well as DPPH and CUPRAC (R^2 = 0.96) assays. The ABTS test was highly correlated with the FRAP test (R^2 = 0.95). The antimicrobial assay proved that each extract had an effect against all bacteria and fungi, except against the bacterium *Pseudomonas aeruginosa*. The highest antibacterial activities were found for methanol extract and ethyl acetate extract against *Staphylococcus aureus*. The highest antifungal activity was observed for the ethyl acetate extract against both *Candida albicans* and *Aspergillus brasiliensis*.

Keywords: Origanum heracleoticum, total phenolic content, antioxidant capacity, antimicrobial activity

[*] Corresponding author: jovana.ickovski@pmf.edu.rs

Introduction

One of the members of the Lamiaceae (Labiatae) family of plants is the genus *Origanum. Origanum* has been largely used in traditional medicine. A strong interest is devoted to it, due to the scientific results, which demonstrate its effectiveness as a source of antioxidant and antimicrobial principles (Carrubba & Calabrese, 1998). The most commonly found oregano species belong to the botanical genus *Origanum*. One of the representatives of this genus is a species *Origanum heracleoticum* L. (syn.: *O. hirtum* L., *O. creticum* Sieber and Bentham, *O. vulgare* L. subsp. *hirtum* (Link) Ietswaart) (Bocchini et al., 1998; Exarchou et al., 2002; Ozcan & Akgul, 1995). *O. heracleoticum* is indigenous to Mediterranean Europe from Spain to northern Balkan and Asia and it is used worldwide in large quantities as a condiment (Lawrence et al., 1974). This subspecies was systematically and widely cultivated in Greece, and it is also known by the vernacular name Greek oregano (Vokou et al., 1993). Oregano has demonstrated antioxidant activity in lipid substrates. Extracts of this herb can retard both the initiation and the rate of lipid oxidation during storage (Tsimogiannis et al., 2006). The essential oil obtained from *O. heracleoticum* plants is characterized by a high phenolic content. The large quantities of carvacrol, thymol, and their precursors, *γ*-terpinene and *p*-cymene (Poulose & Croteau, 1978) characterized all "oregano" types of essential oils (Kokkini et al., 1997). Essential oil is mainly used in the pharmaceutical and food industries (Lawless, 1996). It is also applied in aromatherapy for asthma, bronchitis, rheumatism, and digestive problems. This oil is considered to be cytotoxic (Sivropolou et al., 1996). Chemical analysis of the oregano essential oil revealed the presence of several ingredients, most of which have important antioxidant, antibacterial, and antifungal properties (De Martino et al., 2009; De Souza et al., 2009; Tsimogiannis et al., 2006; Zheng et al., 2009). Very high carvacrol content that was found in a biotype of *O. heracleoticum* is particularly relevant, since this species is known – according to the USA Cancer Chemotherapy National Service Center – to have high antitumoral activity (Baricevic, 1996). Up to now, the *O. heracleoticum* essential oil was the subject of many studies because of all above-mentioned characteristics, while there are only hints of working with Greek oregano extracts. Lamaison et al. (1990, 1993) extensively studied the antioxidant activity of members of Lamiaceae and reported that the content of rosmarinic acid and of total hydroxycinnamic derivatives in hydroalcoholic extracts of *O. vulgare* ssp. *hirtum* was only partly correlated with their antioxidant effect, estimated by measuring the

free radical scavenger effect on DPPH. The antimicrobial test results showed that the essential oil of *O. heracleoticum* has great potential of antimicrobial activity against bacteria, fungi, and yeast species and therefore can be used as a natural preservative ingredient in the food and/or pharmaceutical industry (Biondi et al., 1993). Ethanol extracts were the subject of some studies which were primarily related to the antioxidant activity of these extracts (Baycheva et al., 2020; Conforti et al., 2011) of Bulgarian flora to attenuate oxidative stress effects formed under short-term UV-B radiation.). To the best of our knowledge, this is the first report regarding the total phenolic content, antioxidant and antimicrobial activities of hexane, diethyl ether, ethyl acetate, and methanol extracts of *Origanum heracleoticum* L.

Experimental

Chemicals and reagents

Folin-Ciocalteu's phenol reagent, ABTS, 2,2-diphenyl-1-picrylhydrazyl (DPPH), $FeCl_3$, ascorbic acid, gallic acid, neocuproine, hexane, diethyl ether, ethyl acetate, and methanol were purchased from Sigma Co. (St. Louis, Missouri, USA). 6-Hydroxy-2,5,7,8-tetramethylchroman-2-carboxylic acid (Trolox) was purchased from Acros Organics (Morris Plains, New Jersey, USA). TPTZ (2,4,6-tripyridyl-*s*-triazine), $K_3(Fe(CN)_6)$, phosphate buffer (NaH_2PO_4-Na_2HPO_4; pH 6.6), trichloroacetic acid, HCl, acetate buffers (pH 3.6 and pH 7), Na_2CO_3, $K_2S_2O_8$, $CuCl_2x2H_2O$, and $FeSO_4x7H_2O$, were purchased from Merck (Darmstadt, Germany). All the chemicals and reagents were of analytical purity.

Plant material and plant material extraction

The plant material (*Origanum heracleoticum* L.) was collected at bloom stage on August 2013 on location Berilovac (surroundings of the town of Pirot, Serbia); a voucher specimen 7299 has been deposited in the Herbarium Moesiacum Niš (HMN), Department of Biology and Ecology, Faculty of Science and Mathematics, University of Niš, Serbia. Aerial parts of the herb were used for the experiment. Plants were dried at room temperature and then milled. The ground plant material was packed in a paper bag and kept in a dark, dry, and cool place. The dry plant material (40 g) was extracted with hexane, diethyl ether, ethyl acetate, and methanol (400 mL), by the method of maceration. The resulting mixture was kept for 72 hours in the dark, at room

temperature, with occasional shaking. The resulting extracts were filtered and concentrated on a rotary vacuum evaporator to dryness. The solutions of specified concentrations were made from dried residues for the determination of antioxidant and antimicrobial activity.

Determination of antioxidant activity

Dry extracts were dissolved in methanol (1:1) and the resulting solutions were used for testing the antioxidant activity. All spectrophotometric measurements of the antioxidative potential of *O. heracleoticum* L. extracts were performed on a UV-visible spectrophotometer Perkin Elmer lambda 15 (Massachusetts, USA). Experiments for all assays listed below were performed in three independent repetitions. The mean values of the measurements are presented.

Determination of total phenolic content (TPC)

The total phenolic content of the extracts was determined spectrophotometrically using Folin–Ciocalteu reagent according to the method of Singleton (Singleton et al., 1999). A specified volume of the extract was mixed with 0.625 mL of Folin–Ciocalteu reagent and 2.5 ml of sodium carbonate solution (20%) and the reaction mixture was diluted with distilled water to a total volume of 10 mL. The mixture was shaken and stored in the dark for 30 min. Subsequently, the coloration of the samples was measured at an absorbance of 760 nm using a spectrophotometer. Gallic acid was used as the standard for the calibration curve. The total phenolic content was expressed as gallic acid equivalent per milligram of dry extract weight (μg GAE/mg dw).

2,2-Diphenyl-1-picrylhydrazyl radical scavenging activity (DPPH)

Free radical scavenging activity was determined using the stable 2,2-diphenyl-1-picrylhydrazyl (DPPH) radical according to the method of Hatano (Hatano et al., 1988). The appropriate amounts of extracts were mixed with 2.5 mL of DPPH solution and methanol was added to a total volume of 10 mL. The mixtures were stirred and left to stand in the dark for 1h. The absorbance of the solution was measured at 515 nm. Trolox was used as standard. The free radical capacity toward DPPH radical was determined based on the Trolox calibration curve and the results were expressed as micrograms of Trolox equivalents per milligram of dry extract weight (μg TE/mg dw).

$ABTS^{\bullet+}$ radical cation decolorization assay (ABTS)

The method used for the determination of the antioxidant free radical capacity was the $ABTS^{\bullet+}$ (radical cation) decolorization assay (Re et al., 1999). A stock solution of $ABTS^{\bullet+}$radical cation was prepared by mixing ABTS solution and potassium persulfate solution (1:1). The mixture was maintained in the dark at room temperature for 12 h before use. The working $ABTS^{\bullet+}$solution was produced by dilution of the stock solution in methanol to achieve an absorbance value of 0.7 ±0.02 at 734 nm. An aliquot of diluted extract was poured into $ABTS^{\bullet+}$ working solution (1.8 mL) and methanol was added to a volume of 5 mL. Methanol was used as a referent solution and for the standard calibration curve, Trolox solution was utilized. Absorbance was measured using UV-visible spectrophotometer at 734 nm immediately after addition and mixing and then every minute for 6 min. The radical scavenging capacity of extracts was quantified as micrograms of Trolox equivalents per milligram of dry extract weight (μg TE/mg dw).

Ferric reducing antioxidant power (FRAP)

The ferric reducing antioxidant power (FRAP) assay was based on the methodology of Benzie and Strain (Benzie & Strain, 1996). FRAP reagent was prepared by combining TPTZ with ferric chloride and acetate buffer (1:1:10). The samples were mixed with FRAP reagent (1.0 mL) and water was added to a total volume of 5 mL. Solutions stood for 5 min at 37°C and the absorbance was determined at 595 nm, using methanol as a referent solution. Ferrous ion solution was used as a standard for the calibration curve and FRAP values were expressed as micromoles Fe^{2+} per mg of dry extract weight (μmol Fe/mg dw).

Total reducing power (TRP)

The capacity of extracts to reduce iron (III) to iron (II) was determined according to the method of Oyaizu (Oyaizu, 1986). Reducing power of the extracts was expressed by reducing power of ascorbic acid as a standard antioxidant (AEAC- Ascorbate Equivalent Antioxidant Capacity). The sample (1 mL) was mixed with 2.5 mL of potassium hexacyanoferrate III (1%) and 2.5 mL of phosphate buffer (pH 6.6). After 30 min of incubation at 50 ºC in the dark, 2.5 mL trichloroacetic acid (10%) and 1.5 mL ferric chloride was added. The total volume with the addition of water was 10 mL. The absorbance was measured at 700 nm in a spectrophotometer. Negative (methanol) and positive (ascorbic acid) control reactions were performed, to plot the

absorbance of ascorbic acid against concentration. The results were quantified as mg of ascorbic acid per mg of dry extract weight (mg AAE/mg dw).

Cupric reducing antioxidant capacity assay (CUPRAC)

Cupric reducing antioxidant capacity assay was used for determining antioxidants and hydroxyl radical scavengers, according to the method of Apak (Apak et al., 2004). The reaction mixture was prepared by mixing a specified volume of the extract, 1 mL of neocuproine solution, 1 mL of ammonium acetate buffer (pH 7), 1 mL of copper (II) chloride solution, and distilled water to a total volume of 5 mL. After staying at room temperature for 30 min, the absorbance of the solution was measured at a wavelength of 450 nm. In the same manner, the absorbance of a series of Trolox solutions was determined and the obtained results were used for drafting the calibration curve. The results of the CUPRAC method were expressed as Trolox equivalent per milligram of dry extract weight (mg TE/mg dw).

Antimicrobial activity

The *in vitro* antimicrobial activities of hexane, diethyl ether, ethyl acetate, and methanol extracts of *O. heracleoticum* L. were tested against a panel of laboratory control strains belonging to the American Type Culture Collection (ATCC; Gaithersburg, Maryland, USA) except *S. abony*, belonging to National Collection of Type Cultures (NCTC, Public Health England, London, United Kingdom). Antibacterial activity was evaluated against two gram-positive and three gram-negative bacteria. The gram-positive bacteria used were *Bacillus subtilis* (ATCC 6633) and *Staphylococcus aureus* (ATCC 6538). The gram-negative bacteria utilized in the assay were: *Escherichia coli* (ATCC 8739), *Pseudomonas aeruginosa* (ATCC 9027), and *Salmonella abony* (NCTC 6017). The antifungal activity was tested against two fungal organisms *Aspergillus brasiliensis* (ATCC 16404) and *Candida albicans* (ATCC 10231). Fresh suspensions of microorganisms were prepared from cultures of microorganisms that were kept on agar slants. Extract solutions were made by dissolving 100 mg of dry extract in 1 ml of methanol and the resulting solutions were stored in sealed vials.

Disc-diffusion method

A disc-diffusion method was employed for the determination of the antimicrobial activity of the extracts, according to National Committee for Clinical Laboratory Standards (NCCLS, 1997). The inoculates of the bacterial and fungal strains were prepared from overnight broth cultures and suspensions were adjusted to 0.5 McFarland standard turbidity. A volume of 100 µL of the suspension containing 1.0 x 10^8 CFU/mL of bacteria and 1.0 x 10^4 CFU/mL of fungal spores spread on Mueller-Hinton agar (Torlak, Serbia) and Sabouraud dextrose agar (Torlak, Serbia) respectively, in sterilized Petri dishes (90 mm in diameter) making the 4 mm layer. The discs (12.7 mm in diameter, "Antibiotica Test Blattchen"-Schleicher and Schull, Dassel, Germany) were impregnated with 50 µL of extracts (conc. 100 mg/mL) and placed on the inoculated agar. Negative controls were prepared using methanol. Chloramphenicol (30 µg, Torlak), cefalexin (30 µg, Torlak), and Nystatin (30 µg, Torlak) were used as positive reference standards to determine the sensitivity of a strain of each tested microbial species. The inoculated plates were kept at 4°C for 2 h and incubated at 37°C (24 h) for bacterial strains and at 28°C (48 h) for fungal strains. The antimicrobial activity was evaluated by measuring (in millimeters) the zone of inhibition against the test microorganisms using the appliance "Fisher-Lilly Antibiotic Zone Reder" (Fisher Scientific Co., USA). All microorganisms were completely insusceptible to the control discs imbued with methanol (negative control). The antimicrobial assay was performed in triplicate and the mean values were reported.

Statistical analysis

To examine the interrelationships between the investigated samples, the results were mutually correlated using cluster and linear regression analyses. Cluster Analyses (CA) were carried out with the data of total phenolic content and antioxidant activity to identify various groups. The CA produced a dendrogram using Ward´s method of hierarchical clustering, based on the Euclidean distance between assays. All computations were done using the Statistica 8 software (StatSoft, Tulsa, Oklahoma, USA).

Results and Discussion

The total phenolic content of hexane, diethyl ether, ethyl acetate, and methanolic extracts, calculated from the calibration curve ($R^2 = 0.9951$), expressed as µg gallic acid equivalents/mg is presented in Table 1. The highest total phenolic content was in diethyl ether and methanolic extract (848.5 µg GAE/mg and 733.4 µg GAE/mg, respectively). Higher phenolic content in those extracts, compared to those of hexane and diethyl ether extracts can be a consequence of the different polarity of the extraction solvent (Zhou & Yu, 2004). The analysis of the antioxidant activity of *O. heracleoticum* was performed using five methods: DPPH, ABTS, TRP, FRAP, and CUPRAC, which are distinguished by their mechanism of action. The results of the analysis, represented in Table 1, can vary as a result of the solvent nature and particularly methods of analysis. Results of *in vitro* antioxidant tests give the basic impression of the relative antioxidant activity of *O. heracleoticum* extracts. In general, methanolic and ethyl acetate extracts have higher antioxidant activity than hexane and diethyl ether extracts. This could be the result of a higher total phenolic content in those extracts.

Table 1. Total phenolic (TPC) content, and antioxidant activity (DPPH, ABTS, TRP, FRAP and CUPRAC assays) of *O. heracleoticum* solvent extracts

Extract	**TPC** (µg GAE/mg)	**DPPH** (µg TE/mg)	**ABTS** (µg TE/mg)	**TRP** (mg AAE/mg)	**FRAP** (µmol Fe/mg)	**CUPRAC** (mg TE/mg)
Hexane	532.10	23.40	104.77	49.04	110.32	125.26
Diethyl ether	568.05	37.59	105.13	49.53	151.58	147.28
Ethyl acetate	848.48	47.60	105.48	50.03	189.47	155.92
Methanol	733.43	53.44	106.56	59.44	225.68	155.32

Statistical analysis

Results of the correlation between the total phenolic content and antioxidant activities of *O. heracleoticum* extracts are presented in Table 2. The highest correlation was found between DPPH and FRAP ($R^2 = 0.99$), as well as DPPH and CUPRAC ($R^2 = 0.96$) assays and consequently between FRAP and CUPRAC ($R^2 = 0.90$) tests. The ABTS test was highly correlated with the FRAP test ($R^2 = 0.95$). The ABTS method also showed a high correlation with the DPPH test ($R^2 = 0.89$), as well as with the TRP assay ($R^2 = 0.95$). Such a high correlation may be explained by the fact that all four assays (DPPH, FRAP, ABTS, and CUPRAC) are electron transfer methods. Minimum interdependence was observed between the total phenolic content and the total reducing power assay ($R^2 = 0.35$), which can be explained by the fact that phenols are not the only class of

compounds that may affect the total reduction potential of the examined extracts. The correlation coefficients of TPC with DPPH and CUPRAC assays are 0.82 and 0.80, respectively, suggesting that phenolic compounds are likely to contribute to the radical scavenging activity of the plant.

Table 2. Correlation coefficients between TPC and the results of antioxidant assays (DPPH, ABTS, TRP, FRAP, CUPRAC)

	TPC	DPPH	ABTS	FRAP	TRP	CUPRAC
TPC	1.00	0.82	0.59	0.78	0.35	0.80
DPPH		1.00	0.89	0.99	0.71	0.96
ABTS			1.00	0.95	0.95	0.73
FRAP				1.00	0.81	0.90
TRP					1.00	0.51
CUPRAC						1.00

Cluster analysis was used to classify *O. heracleoticum* extracts (objects) based on a set of measured antioxidant activities (variables) into several different groups (clusters). In the case of agglomerative hierarchical cluster analysis, a dissimilarity matrix was used. The elements of this matrix were the Euclidean distances as the measure of similarity/dissimilarity and complete linkage as the agglomerative method. To obtain clusters, Ward's method was used. This agglomerative method considers each sample as a separate cluster, there are as many clusters as samples and then combines the clusters sequentially, reducing the number of clusters at each step until only one cluster is left. The clusters are linked at increasing levels of dissimilarity (Rencher, 2003). The linkage distance is shown as D_{link}/D_{max}, which represents the quotient between the linkage distances for a particular case divided by the maximal linkage distance.

The dendrogram of the AHC analysis, with two statistically different classes, is given in Fig. 1. According to this, FRAP, CUPRAC, and ABTS (the same cluster) are mutually similar while TRP and DPPH form separate classes. The results of the correlation analysis to some extent coincide with the results of the AHC analysis in the part of good correlation between FRAP and ABTS, that is, FRAP and CUPRAC tests, while there are noticeable discrepancies between these two statistical methods in the part of the correlation of ABTS and CUPRAC, as well as DPPH and TRP methods.

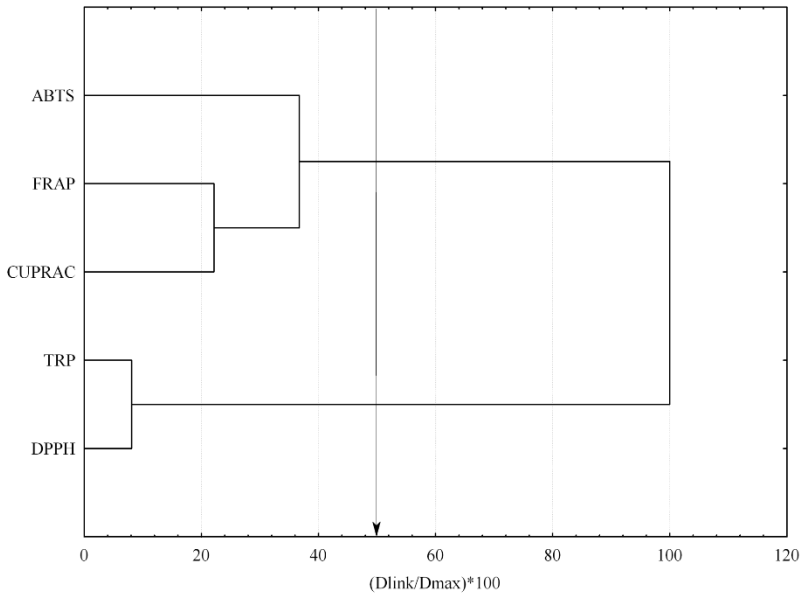

Figure 1. Dendrogram obtained by agglomerative hierarchical clustering of antioxidant potential (determined by five different methods: DPPH, ABTS, TRP, FRAP, and CUPRAC) of four *O. heracleoticum* solvent extracts

The antimicrobial activity of the solvent extracts against five bacteria and two fungi species was assessed using the disc-diffusion method. The results are presented in Table 3. The studied samples showed good antimicrobial potential, none of the samples exhibited very low activity against tested microorganisms, except against *P. aeruginosa*; none of the extracts showed any activity against *P. aeruginosa*. All samples showed almost equal activity against *E. coli*. The same was observed with extracts against *S. abony*, as well. Only the ethyl acetate extract was slightly more active against *S. abony* in comparison to other samples. In the case of Gram-positive bacteria, all examined extracts exhibited strong activity against *S. aureus*, methanol extract and ethyl acetate extract evinced the highest activity. All tested samples (5 mg of each) showed different diameters of inhibition zone against *B. subtilis*. The highest value was measured for methanol extract. Anti-*C. albicans* activity of the extracts was very high, the highest was for ethyl acetate extract. Also, all tested samples, except hexane extract, showed significantly high anti-*A. brasiliensis* activity; ethyl acetate extract was again the most active one.

Table 3. The results of the antimicrobial activity testing (inhibition zones presented in millimeters including disk diameter)

Extract	Gram-negative bacteria			Gram-positive bacteria		Fungi	
	E. coli	*S. abony*	*P. aeruginosa*	*S. aureus*	*B. subtilis*	*C. albicans*	*A. brasiliensis*
Hexane extract	21	19	/	50	25	36	17
Diethyl ether extract	21	20	/	60	27	38	35
Ethyl acetate extract	20	25	/	65	31	50	47
Methanol extract	24	19	/	65	35	42	44
Methanol	/	/	/	/	/	/	/
Cephalexin	19	18	/	36	39	nt	nt
Chloramphenicol	22	25	12	30	29	nt	nt
Nystatin	nt	nt	nt	nt	nt	18	17

/ - not detected, nt - not tested

Conclusion

The highest total phenolic content was found in ethyl acetate extract and methanol extract. Higher phenolic content in those extracts, compared to those of hexane and diethyl ether extracts is a consequence of different solvent polarity. The examination of antioxidant activity showed that methanol and ethyl acetate extracts had the strongest activity, and this is the result of a higher total phenolic content in those extracts, than in hexane and diethyl ether extracts. Anti-*C. albicans* activity of the extracts was very high, the highest was for ethyl acetate extract. All tested samples, except hexane extract, showed significantly high anti-*A. brasiliensis* activity. To the best of our knowledge, this is the first report regarding total phenolic content, antioxidant and antimicrobial activities of hexane, diethyl ether, ethyl acetate, and methanol extracts of *Origanum heracleoticum* L.

Acknowledgments

This work was funded by the Ministry of Education, Science and Technological Development of Serbia (Project No. 451-03-47/2023-01/ 200124) and the Serbian Academy of Sciences and Art (SASA), Branch of SASA in Nis (Project No. 0-13-18).

References

Apak, R., Güçlü, K., Özyürek, M., & Karademir, S.E. (2004). Novel total antioxidant capacity index for dietary polyphenols and vitamins C and E, using their cupric ion reducing capability in

the presence of neocuproine: CUPRAC method. Journal of Agricultural and Food Chemistry, 52, 7970-7981.

Baricevic, D. (1996). Experiences with oregano (*Oreganum* spp.) in Slovenia, in: Proceedings of the IPGRI International Workshop on Oregano, CIHEAM, Valenzano, Bari, Italy.

Baycheva, S. K., Karamalakova, Y. D., Nikolova, G. D., Dobreva, K. Z., & Gadjeva, V. G. (2020). An ethanol extract ability of cultivated white oregano (*Origanum heracleoticum* L.) of Bulgarian flora to attenuate oxidative stress effects formed under short-term UV-B radiation. Bulgarian Chemical Communications, 52, 118-124.

Benzie, I. F. F., & Strain, J. J. (1996). The ferric reducing ability of plasma (FRAP) as a measure of "Antioxidant Power": The FRAP assay. Analytical Biochemistry, 239, 70-76.

Biondi, D., Cianci, P., Geraci, C., Ruberto, G., & Piattelli, M. (1993). Antimicrobial activity and chemical composition of essential oils from sicilian aromatic plants. Flavour and Fragrance Journal, 8, 331–337.

Bocchini, P., Russo, M., & Galletti, G.C. (1998). Pyrolysis-gas chromatography/mass spectrometry used as a microanalytical technique for the characterization of *Origanum heracleoticum* from Calabria, southern Italy. Rapid Communications in Mass Spectrometry, 12, 1555-1563.

Carrubba, A., & Calabrese, I. (1998). Antioxidant compounds in some herbaceous aromatic plants. Acta Horticulturae, 457, 85-93.

Conforti, F., Marrelli, M., Menichini, F., Tundis, R., Statti, G. A., Solimene, U., & Menichini, F. (2011). Chemical composition and protective effect of oregano (*Origanum heracleoticum* L.) ethanolic extract on oxidative damage and on inhibition of NO in LPS-stimulated RAW 264.7 macrophages. Journal of Enzyme Inhibition and Medicinal Chemistry, 26(3), 404-411.

De Martino, L., De Feo, V., Formisano, C., Mignola, E., & Senatore, F. (2009). Chemical composition and antimicrobial activity of the essential oils from three chemotypes of *Origanum vulgare* L. ssp. *hirtum* (Link) letswaart growing wild in Campania (Southern Italy). Molecules, 14, 2735-2746.

De Souza, E.L., de Barros, J.C., da Conceição, M.L., Gomes Neto, N.J.G., & da Costa, A.C.V. (2009). Combined application of *Origanum vulgare* L. Essential oil and acetic acid for controlling the growth of *Staphylococcus aureus* in foods. Brazilian journal of Microbiology, 40, 387-393.

Exarchou, V., Nenadis, N., Tsimidou, M., Gerothanassis, I.P., Troganis, A., & Boskou, D. (2002). Antioxidant activities and phenolic composition of extracts from Greek oregano, Greek sage, and summer savory. Journal of Agricultural and Food Chemistry, 50, 5294–5299.

Hatano, T., Kagawa, H., Yasuhara, T., & Okuda, T. (1988). Two new flavonoids and other constituents in licorice root: their relative astringency and radical scavenging effects. Chemical and Pharmaceutical Bulletin, 36, 2090–2097.

Kokkini, S., Karousou, R., Dardioti, A., Krigas, N., & Lanaras, T. (1997). Autumn essential oils of Greek oregano. Phytochemistry, 44, 883–886.

Lamaison, J.L., Petitjean-Freytet, C., & Carnat, A. (1990). Rosmarinic acid, total hydroxycinnamic derivatives and antioxidant activity of Apiaceae, Borraginaceae and Lamiceae medicinals. Annales Pharmaceutiques Françaises, 48, 103-108.

Lamaison, J.L., Petitjean-Freytet, C., Duke, J.A., & Walker, J. (1993). Hydroxycinnamic derivative levels and antioxidant activity in North American Lamiaceae. Plantes Medicinales Et Phytotherapie 26, 143-148.

Lawless, J. (2002). The Encyclopaedia of Essential Oils. London: Thorsons.

Lawrence, B.M., Terhlne, S.J., & Hocc, J.W. (1974). 4,5-Epoxy-*p*-Menth-1-ene: A new Constituent of *Origanum Heracleoticum*. Phytochemistry, 13, 1012-1013.

NCCLS, (National Committee for Clinical Laboratory Standards). (1997). M2-A6 Performance standards for antimicrobial disk susceptibility testing; 6th International Supplement, Wayne, PA.

Oyaizu, M. (1986). Studies on products of browning reaction. Antioxidative activities of products of browning reaction prepared from glucosamine. The Japanese Journal of Nutrition and Dietetics, 44, 307-315.

Özcan, M., & Akgül, A. (1995). Capers (*Capparis spp*.): composition and pickling Product. Workshop - Medicinal and Aromatic Plants, Ege. Univ. Agric. Fac., Bornova-Ýzmir, Turkey.

Poulose, A.J., & Croteau, R. (1978). Biosynthesis of aromatic monoterpenes: Conversion of γ-terpinene to *p*-cymene and thymol in *Thymus vulgaris* L. Archives of Biochemistry and Biophysics, 187, 307-314.

Re, R., Pellegrini, N., Proreggente, A., Pannala, A., Yang, M., & Rice-Evans, C. (1999). Antioxidant activity applying an improved ABTS radical cation decolorization assay. Free Radical Biology and Medicine, 26, 1231-1237.

Rencher, A.C. (2003). Methods of multivariate analysis. (Vol. 492). John Wiley & Sons.

Singleton, V. L., Orthofer, R., & Lamuela-Raventós, R. M. (1999). Analysis of total phenols and other oxidation substrates and antioxidants by means of folin-ciocalteu reagent. Methods in Enzymology, 299, 152-178.

Sivropoulou, A., Papanikolaou, E., Nikolaou, C., Kokkini, S., Lanaras, T., & Arsenakis, M. (1996). Antimicrobial and cytotoxic activities of *Origanum* essential oils. Journal of Agricultural and Food Chemistry, 44(5), 1202-1205.

Tsimogiannis, D., Stavrakaki, M., & Oreopoulou, V. (2006). Isolation and characterisation of antioxidant components from oregano (*Origanum heracleoticum*). International Journal of Food Science & Technology, 41, 39-48.

Vokou, D., Kokkini, S., & Bessière, J.-M. (1993). Geographic variation of Greek oregano (*Origanum vulgare* ssp. *hirtum*) essential oils. Biochemical Systematics and Ecology, 21, 287-295.

Zheng, Z. L., Tan, J. Y. W., Liu, H. Y., Zhou, X. H., Xiang, X., & Wang, K. Y. (2009). Evaluation of oregano essential oil (*Origanum heracleoticum* L.) on growth, antioxidant effect and resistance against *Aeromonas hydrophila* in channel catfish (*Ictalurus punctatus*). Aquaculture, 292(3-4), 214-218.

Zhou, K., & Yu, L. (2004). Effects of extraction solvent on wheat bran antioxidant activity estimation. Food Science and Technology, 37, 717-721.

Ukupni sadržaj fenola, antioksidativni kapacitet, i antimikrobna aktivnost *Origanum heracleoticum* L., ekstrahovanog različitim rastvaračima

Jovana D. Ickovski[1], Ivan R. Palić[1], Aleksandra S. Đorđević[1], Vesna P. Stankov Jovanović[1], Violeta D. Mitić[1], Gordana S. Stojanović[1]

1-Univerzitet u Nišu, Prirodno-matematički fakultet, Departman za hemiju, Višegradska 33, 18000 Niš, Srbija

SAŽETAK

Ovo istraživanje je zasnovano na ispitivanju ukupnog sadržaja fenola, antioksidativne i antimikrobne aktivnosti heksanskog, dietil etarskog, etil acetatnog i metanolnog ekstrakta *Origanum heracleoticum* L. koji je sakupljen u Srbiji. Antimikrobna aktivnost je testirana na pet bakterija i dve gljivice metodom disk difuzije. Određen je ukupan sadržaj fenola u ekstraktima *O. heracleoticum* i korišćeno je pet različitih testova za skrining antioksidativnog kapaciteta. Najveći ukupni sadržaj fenola utvrđen je u etilacetatnom ekstraktu (848.48 mg GAE/mg suvog ekstrakta) i metanolnom ekstraktu (733.43 mg GAE/mg suvog ekstrakta). Ispitivanje antioksidativne aktivnosti pokazalo je da su najjaču aktivnost imali metanolni i etil acetatni ekstrakti. Najbolja korelacija je pronađena između DPPH i FRAP (R^2 = 0.99), kao i DPPH i CUPRAC (R^2 = 0.96) testova. ABTS test je bio u visokoj korelaciji sa FRAP testom (R^2 = 0.95). Antimikrobni test je pokazao da je svaki ekstrakt aktivan protiv svih ispitivanih bakterija i gljivica, osim protiv bakterije *Pseudomonas aeruginosa*. Najveća antibakterijska aktivnost pronađena je za metanolni ekstrakt i etil acetatni ekstrakt protiv *Staphilococcus aureus*. Najveća antifungalna aktivnost primećena je za etil acetatni ekstrakt protiv *Candida albicans* i za metanolni ekstrakt protiv *Aspergillus brasiliensis*.

Ključne reči: Origanum heracleoticum, ukupni sadržaj fenola, antioksidativni kapacitet, antimikrobna aktivnost

Teneur phénolique totale, capacité antioxydante et activité antimicrobienne d'*Origanum heracleoticum* L., extrait avec différents solvants

Jovana D. Ickovski[1], Ivan R. Palić[1], Aleksandra S. Đorđević[1], Vesna P. Stankov Jovanović[1], Violeta D. Mitić[1], Gordana S. Stojanović[1]

1-Université de Niš, Faculté des sciences naturelles et des mathématiques, Département de chimie, Višegradska 33, 18000 Niš, Serbie

RÉSUMÉ

Cette recherche était basée sur l'examen de la teneur phénolique totale, des activités antioxydantes et antimicrobiennes de l'hexane, de l'éther diéthylique, de l'acétate d'éthyle et des extraits de méthanol d'*Origanum heracleoticum* L. cultivés en Serbie. L'activité antimicrobienne a été déterminée contre cinq bactéries et deux champignons à l'aide de la méthode de diffusion sur disque. La teneur phénolique totale des extraits de solvants *d'O. heracleoticum* a été déterminée et cinq tests différents ont été utilisés pour le dépistage de la capacité antioxydante. La plus grande teneur phénolique totale a été trouvée dans l'extrait d'acétate d'éthyle (848.48 µg GAE/mg d'extrait sec) et l'extrait de méthanol (733.43 µg GAE/mg d'extrait sec). L'examen de l'activité antioxydante a montré que les extraits de méthanol et d'acétate d'éthyle avaient la plus forte activité. La corrélation la plus élevée a été trouvée entre DPPH et FRAP ($R^2 = 0.99$), ainsi qu'entre les tests DPPH et CUPRAC ($R^2 = 0.96$). Le test ABTS était fortement corrélé avec le test FRAP ($R^2 = 0.95$). Le test antimicrobien a prouvé que chaque extrait avait un effet contre toutes les bactéries et les champignons, sauf contre la bactérie *Pseudomonas aeruginosa*. L'activité antibactérienne la plus élevée a été trouvée pour l'extrait de méthanol et l'extrait d'acétate d'éthyle contre *Staphylococcus aureus*. L'activité antifongique la plus élevée a été observée pour l'extrait d'acétate d'éthyle contre *Candida albicans* et pour l'extrait de méthanol contre *Aspergillus brasiliensis*.

Mots-clés: Origanum heracleoticum, teneur phénolique totale, capacité antioxydante, activité antimicrobienne

Общее содержание фенола, антиоксидантная способность, и антимикробная активность *Origanum heracleoticum* L., извлеченная различными растворителями

Йована Д. Иковский[1], Иван Р. Палич[1], Александра С. Джорджевич[1], Весна П. Станков Йованович[1], Виолетта Д. Митич[1], Гордана С. Стоянович[1]

1-Нишский университет, Естественно-математический факультет, кафедра химии, Вышеградская 33, 18000 Ниш, Сербия

Резюме

Это исследование было основано на изучении общего содержания фенола, антиоксидантной и антимикробной активности экстракта гексана, диэтилового эфира, этилацетата и метанола *Origanum heracleoticum* L., который был собран в Сербии. Антимикробную активность тестировали на пяти бактериях и двух грибках методом дисковой диффузии. Было определено общее содержание фенола в экстрактах *O. heracleoticum* и были использованы пять различных тестов для скрининга антиоксидантной способности. Наибольшее общее содержание фенола было обнаружено в экстракте этилацетата (848, 48 мг GAE/мг сухого экстракта) и экстракте метанола (733, 43 мг GAE/мг сухого экстракта). Исследование антиоксидантной активности показало, что метанольные и этилацетатные экстракты обладают наибольшей активностью. Наилучшая корреляция была обнаружена между тестами DPPH i FRAP (R^2 = 0.99), а также тестами DPPH и CUPRAC (R^2 = 0.96). Тест ABTS сильно коррелировал с тестом FRAP (R^2 = 0.95) Антимикробный тест показал, что каждый экстракт активен против всех исследованных бактерий и грибков, за исключением бактерии *Pseudomonas aeruginosa*. Наибольшая антибактериальная активность была выявлена для экстракта метанола и экстракта этилацетата против *Staphilococcus aureus*. Наибольшая противогрибковая активность наблюдалась у экстракта этилацетата против *Candida albicans* и у экстракта метанола против *Aspergillus brasiliensis*.

Ключевые слова: Origanum heracleoticum, общее содержание фенолов, антиоксидантная способность, антимикробная активность

Gesamtphenolgehalt, antioxidative Kapazität und antimikrobielle Aktivität von *Origanum heracleoticum* L., extrahiert mit verschiedenen Lösungsmitteln

Jovana D. Ickovski[1], Ivan R. Palić[1], Aleksandra S. Đorđević[1], Vesna P. Stankov Jovanović[1], Violeta D. Mitić[1], Gordana S. Stojanović[1]

1- Universität Niš, Mathematisch-Naturwissenschaftliche Fakultät, Abteilung für Chemie, Višegradska 33, 18000 Niš, Serbien

ABSTRAKT

Diese Studie untersuchte den Gesamtphenolgehalt, die antioxidative und antimikrobielle Aktivität des hexanischen, diethyletherischen, ethylacetathaltigen und methanolischen Extrakts von *Origanum heracleoticum L.*, das in Serbien gesammelt wurde. Die antimikrobielle Aktivität wurde mit der Scheibendiffusion-Methode gegenüber fünf Bakterien und zwei Pilzen getestet. Der Gesamtphenolgehalt in den Extrakten von *O. heracleoticum* wurde bestimmt und fünf verschiedene Tests wurden zum Screening des antioxidativen Potenzials verwendet. Der höchste Gesamtphenolgehalt wurde im Ethylacetat-Extrakt (848,48 mg GAE/mg Trockenextrakt) und im Methanol-Extrakt (733,43 mg GAE/mg Trockenextrakt) festgestellt. Die Untersuchung der antioxidativen Aktivität zeigte, dass die Methanol- und Ethylacetatextrakte die stärkste Aktivität aufwiesen. Die höchste Korrelation wurde zwischen DPPH und FRAP (R^2 = 0,99) sowie zwischen DPPH und CUPRAC (R^2 = 0,96) Tests festgestellt. Der ABTS-Test zeigte eine hohe Korrelation mit dem FRAP-Test (R^2 = 0,95). Der antimikrobielle Test zeigte, dass jeder Extrakt gegen alle getesteten Bakterien und Pilze aktiv war, mit Ausnahme des Bakteriums *Pseudomonas aeruginosa*. Die höchste antibakterielle Aktivität wurde beim Methanolextrakt und Ethylacetatextrakt gegen *Staphylococcus aureus* festgestellt. Die stärkste antimykotische Aktivität für den Ethylacetatextrakt sowohl gegen *Candida albicans* als auch gegen *Aspergillus brasiliensis* beobachtet.

Schlüsselwörter: Origanum heracleoticum, Gesamtphenolgehalt, antioxidative Kapazität, antimikrobielle Aktivität

Chemia Naissensis, Vol 5, Issue 2, RESEARCH ARTICLE, 54-68 DOI: 10.46793/ChemN5.2.54I

Ripe and unripe seed of *Xanthium italicum* - elemental composition

Marija Ilić[1], Violeta Mitić[2], Jelena Nikolić[2*], Marija Marković[2], Jelena Mrmošanin[2], Aleksandra Pavlović[2], Vesna Stankov Jovanović[2]

1-Specialized veterinary institute, Dimitrija Tucovića 175, Niš, Serbia

2-University of Niš, Faculty of Sciences and Mathematics, Department of Chemistry, Višegradska 33, Niš, Serbia

ABSTRACT

Elements content in plants varies considerably, which is a consequence of various factors, such as plant species, vegetative stage, pedological characteristics of the soil and environmental conditions. The subject of this work is an investigation of the elemental composition of *Xanthium italicum* ripe and unripe seed collected in Temska using ICP OES. Out of the analyzed macroelements, potassium is the one with the highest concentration, and its content significantly differs in the ripe and unripe seeds. Iron showed five times higher concentration in unripe (27.7 µg/g) compared to ripe (6.2 µg/g) seed. The content of Ba, Cr, Cu, Mn, Pb, and Zn also differ in the ripe and unripe stages of the analyzed seed, which indices that elemental composition is affected by the vegetative stage. Lead and arsenic content are higher than permissible limits, which might affect honey production in this region.

Keywords: Xanthium italicum, elemental composition, ICP OES, seed

* Corresponding author: jelena.cvetkovic@pmf.edu.rs

Introduction

Plant usage dates back to the first days of human history. Even today, in the era of great technological achievements, interest in plant usage in pharmacy, medicine, nutrition, as well as in other industries increases. The reason for that is the fact that plants are considered to be biochemical factories, with numerous and diverse products. For a plant to have the practical application it is necessary to know its chemical composition. However, the great natural products potential has not yet been sufficiently studied and used. Thus, chemical composition and product quality research represent an important field of scientific research because it helps to create conditions for successful plant usage, which can be of great importance for the economy and human health.

Xanthium species belong to important weed species, widely distributed, both worldwide and in Serbia. In many countries, they have the character of very important weed species, and in some, they are also classified as invasive species (Anastasiu et al., 2007; Galanos, 2015). They could be poisonous to animals. However, some of them have anticancerogenic effects and inhibit the development of lung and ovarian melanoma cells, as well as the central nervous system and colon (Ramirez-Erosa et al., 2007). It could also be used for the treatment of inflammatory diseases, such as rhinitis, empyema, and rheumatoid arthritis (Yoou et al., 2008).

X. italicum is an annual species, with large dispersion and propagation capacity, 30-100 cm tall, yellow-green, with an aromatic smell. As a weed, *Xanthium italicum* is present in wheat (Novák et al., 2009), sunflower (Manilov & Zhalnov, 2018), potato (Ilić & Nikolić, 2011), cotton (Economou et al., 2005), as well as in rural habitats (Fetvadjieva & Milanova, 1998). Its presence was also recorded in sports and recreational fields (Stevanović et al., 2009), indicating the great adaptability of *Xanthium* species and their potential to spread and persist in highly unstable plant communities. Its potential benefit could be reflected in the fact that it belongs to honey plants (Zima & Štefanić, 2018). *X. italicum* also possesses allelopathic activity, because xanthosine from its fruit reduces the germination of some weed seed species (Shao et al., 2012).

The chemical composition of plants is mostly affected by plant species, environmental composition and plant maturity. Previous studies on the biochemical composition of various plants fruits (Izonfuo & Omuaru, 1988; Baiyeri, 2000; Baiyeri and Unadike, 2001) reported that nutrient

composition is significantly affected by plant maturity. Baiyeri (2000) found higher doses of N, P, K, Mg and Ca in ripe plantain pulp compared to unripe but lower Fe, Cu, Zn and Na concentrations in ripe fruits.

This study aimed to investigate the content of Al, As, B, Ba, Be, Ca, Cd, Co, Cr, Cu, Fe, K, Mg, Mn, Na, Ni, P, Pb, Si and Zn content in *Xanthium italicum* ripe and unripe seed using ICP OES. After the elemental composition is determined, differences in their content are studied to point out if the vegetative stage affects it. As far as we know, this is the first time ripe and unripe seed was analyzed.

Experimental

Plant and soil material

X. italicum plant was collected around the village of Temska. Samples were air-dried, homogenized and stored at 4°C until analysis.

Chemicals and instruments

Hydrochloric acid, nitric acid (65%), and hydrogen peroxide (30%), were purchased from Merck (Darmstadt, Germany). Multi - element standard solutions (20.00 ± 0.10 mg L^{-1}) used for ICP analysis was purchased from Ultra Scientific (North Kingstown, RI, U.S.A.).

The measurements were carried out with an ICP-OES iCAP 6000, Thermo Scientific. Table 1 shows the analytical parameters for ICP-OES.

Table 1. ICP-OES instrumental parameters

Flush Pump Rate	100 rpm
Analysis Pump Rate	50 rpm
Nebulizer gas	0.7 $Lmin^{-1}$
Coolant Gas Flow	12 $Lmin^{-1}$
Auxiliary Gas Flow	0.5 $Lmin^{-1}$
Plasma View	axial
Flush time	30 s

Table 2 shows the selected wavelengths of the investigated elements, limits of detection (LOD), limits of quantification (LOQ) and correlation coefficients of calibration curves (r).

Tabel 2. ICP OES method parameters

Element	λ (nm)	LOD (ppm)	LOQ (ppm)	r
Al	396.1	0.001234	0.004114	0.999625
As	189	0.003263	0.010877	0.999873
B	208.9	0.000982	0.003274	0.998998
Ba	455.4	0.000061	0.000202	1
Be	311.1	0.000435	0.001346	1
Ca	317.9	0.000333	0.001111	0.999927
Cd	226.5	0.000137	0.000456	0.999476
Co	228.6	0.000266	0.000888	0.999453
Cr	267.7	0.000561	0.001871	0.998638
Cu	324.7	0.000426	0.001418	0.999359
Fe	240.4	0.000547	0.001822	0.998834
K	766.4	0.001143	0.003811	0.994010
Mg	280.2	0.000127	0.000425	0.999967
Mn	259.3	0.000082	0.000273	0.998823
Na	589.5	0.000009	0.000031	1
Ni	231.6	0.000422	0.001408	0.999049
P	213.1	0.004049	0.013497	0.999962
Pb	220.3	0.001858	0.006195	0.999684
Si	251.1	0.001897	0.006323	0.999999
Zn	213.8	0.000097	0.000323	0.998704

Sample preparation

An acid digest of plant species was prepared by oxidizing 1 g of sample with conc. HNO_3 and left in the dark for 12 hours. After that, H_2O_2 (30%) and water were added. A digestion procedure was applied to obtained mixtures to reduce the volume and improve decomposition. Another portion of H_2O_2 was added and evaporation continued. After cooling concentrated HCl was added, and the mixture was left overnight. The resulting suspension was filtered and the rest is rinsed with hot HCl and then heated with deionized water. Filtrate was collected in a volumetric flask and diluted (US EPA, 1996). Each sample was analyzed twice, and the data were reported as a mean of the analyzed samples in μg/g.

Statistical analysis

The data were based on two replicates and subjected to statistical analysis in Statistica 8.0 software (StatSoft, Tulsa, Oklahoma, USA). A probability level of $p< 0.05$ was considered statistically significant.

Results and Discussion

All elements can be considered as biologically important elements, toxic and elements that have no biological role, but no toxic effect when reaching the body in small concentrations. However, it is not always easy to distinguish toxic elements from others, as they are all considered to be toxic in higher quantities. Metals can affect a long list of physiological and biochemical processes in plants and their toxicity varies with plant species. The inadequate supply of a nutrient, whether leading to deficiency or toxicity, affects plant growth and results in yield and quality losses in agricultural plants (Brdar-Jokanović, 2020).

Macroelements content

For normal plant growth and development, 17 elements are needed, of which 9 (C, O, H, N, S, Ca, K, Mg and P) are needed in higher amounts (>0.1 %) and these are called macro elements. Macro elements are structural components of tissues with certain functions in cells and metabolism, as well as in water and acid-base balance (Imelouane et al., 2011). The content of macroelements analyzed in *X. italicum* ripe and unripe seed are presented in Table 3.

Tabela 3. Macroelement content in unripe and ripe *X. italicum* seed (µg/g)

Element	Unripe	Ripe
Ca	1173±94[a]	1740±106[b]
Na	13.9±0.9[a]	16.6±0.4[a]
K	9918±66[a]	8813±11[b]
P	5044±83[a]	4347±16[b]
Mg	472±5[a]	483±9[a]

Values followed by the same letter are not significantly different at $p \leq 0.05$ significance.

The element with the highest concentration in the analyzed plant tissue is K with 9918±66 µg/g for unripe and 8813±11 µg/g for ripe seed. Potassium is important for ensuring optimal plant growth (White & Karley, 2010). Changes in potassium content might be explained by its great mobility in plants since it is an important component in protein synthesis and carbohydrate metabolism (Trankner et al., 2018). Phosphorus, an essential nutrient, is a component of the complex nucleic acid structure of plants, which regulates protein synthesis, and it is important in cell division and the development of new tissue. Phosphorus contributes to flower initiation and root, seed, and fruit development. This element is highly mobile in plants, and when deficient, it may be translocated from old plant tissue to young, actively growing areas. As a plant matures,

phosphorus is translocated into the fruiting areas of the plant, where high-energy requirements are needed for the formation of seeds and fruit. Phosphorus content was also higher in unripe (5044±83 μg/g) compared to ripe *X. italicum* seed (4347±16 μg/g).

On the other hand, the content of three other analyzed macroelements (Ca, Na and Mg) is slightly higher in ripe compared to unripe seeds. Differences in Na and Mg content are not significant, whereas Ca content is higher in ripe seed for about 600 μg/g. Paul et al. (2012) concluded that relatively immobile element such as Ca migrates to the fruit at later stages of plant development, which agrees with our results. Calcium as an essential plant nutrient is required for various structural roles in the cell wall and membranes. This secondary nutrient, critical to crop development, is only xylem mobile, meaning it can only move up the plant, and once in place, it cannot be remobilized and moved to new developing tissues.

Among macroelements lowest concentration was recorded for Na (13.9±0.9 and 16.6±0.4 μg/g for unripe and ripe fruit, respectively). Higher plants require sodium to be able to grow to their full potential and increased growth rates. Compared to Chirigiu et al. (2003), macroelement content in analyzed *X. italcium* Mg and Na content was lower in the present study, but K and Ca content was a few times higher in our *X. italicum* seed samples. The reason for that could be environmental conditions and plant maturity, but also different instrumental techniques have been used for elemental analysis.

Microelements content

Microelements are essential elements that are required in relatively small amounts for plants' metabolic processes, and these include iron, manganese, zinc and copper (Wiedenhoeft, 2006). Microelements content in analyzed *X. italicum* seed are presented in Figure 1.

As can be seen from Figure 1, among microelements, an element with the highest concentration in analyzed samples is Fe, for unripe *X. italicum* seed (27.7 μg/g). In the case of ripe seed, Fe content is almost five times lower (6.3 μg/g). For iron adsorption to plant environmental conditions, a high pH value, but also phosphate and Ca^{2+} concentrations, are key factors, which reduce iron mobility from soil to plant. At the vegetative stage, most of the iron is translocated to aerial parts and used for photosynthesis, whereas at the reproductive stage, a large part of the Fe present in vegetative tissues is transferred to the seeds (Mari et al., 2020). Also, its important role is in pectin metabolism

and influences tissue softening during ripening (Bai et al., 2021). However, in the case of *X. italicum* in this study, Fe content is much lower for ripe seed. The content of other analyzed microelements is lower in ripe seeds, compared to unripe ones.

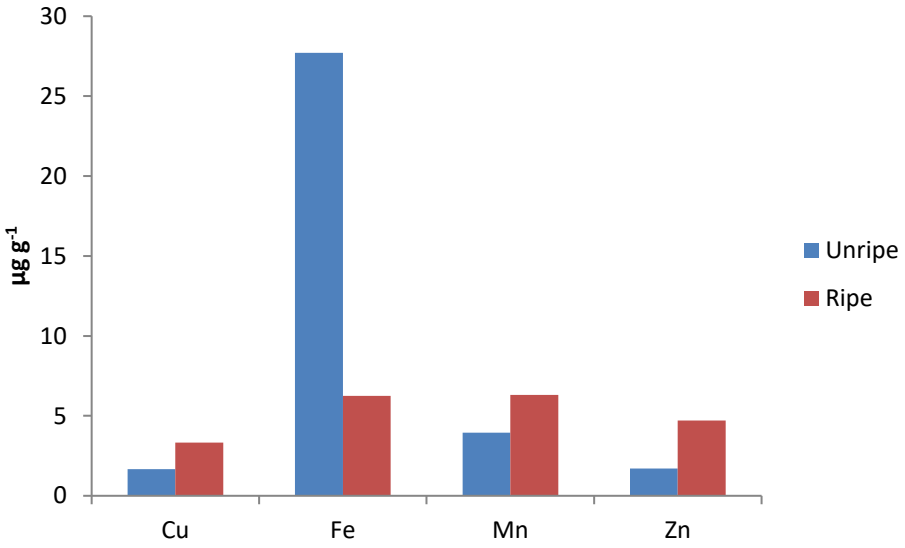

Figure 1. Content of Cu, Fe, Mn and Zn in analyzed *X. italicum* seed

Zinc is an essential element for all living organisms and plays an important role in the biosynthesis of enzymes, auxins, and other proteins in plants. The main signs of Zn toxicity in various plant species are indicated by a decrease in growth and development of the plant, alteration in metabolism processes and induction of oxidative damage (Versieren et al., 2017). Zn concentration is three times lower in ripe (1.7 µg/g) compared to unripe (4.7 µg/g) *X. italicum* seeds (Figure 1). Plants mainly absorb zinc in the form of Zn^{2+} cation, but in alkaline environment in the form of $ZnOH^{+}$ cation; Zn mobility in plants is moderate. Zinc increases the tolerance of plants to diseases. The range of 300-400 mg/kg d.w. is accepted as the toxicity limit for Zn in plants (Kabata-Pendias & Pendias, 1992). Compared to the Zn content of *X. strumarium* (average 0.129 µg/g) analyzed by Tadesse et al. (2018), *X. italicum* from this study had a higher Zn concentration (average 3.2 µg/g). However, Chirigiu et al. (2003) found 31.6 and 32.5 µg/g of Zn in *X. italicum* and *X. spinosum*, respectively, indicating that Zn content is not only affected by plant species but also the geographic origin and atmospheric conditions.

Copper is another essential element for plants and they mainly absorb copper in the form of Cu^{2+} ions and chelates. Excess Cu can cause a lack of other elements, especially manganese and iron. Studies have shown that plants that have high concentrations of oxygen and phosphorus are generally characterized by a low concentration of copper. Copper mobility in plants is medium and the first defects appear on the youngest organs. Twice a higher concentration of Cu is recorded in ripe (3.3 µg/g) compared to unripe seed (1.7 µg/g) (Figure 1).

Among microelements, there are ones with known biological function in plants, as well as ones with no function or toxic ones. For example, Zn, Ni, Cu, V, Co, W and Cr are considered to be toxic elements, but also essential in trace amounts, while As, Hg, Ag, Sb, Cd, Pb and U, have no known beneficial role and they are toxic to plants. Content of Al, As, B, Ba, Be, Cd, Co, Cr, Ni, Pb and Si content in analyzed *X. italicum* ripe and unripe seeds is presented in Figures 2 and 3.

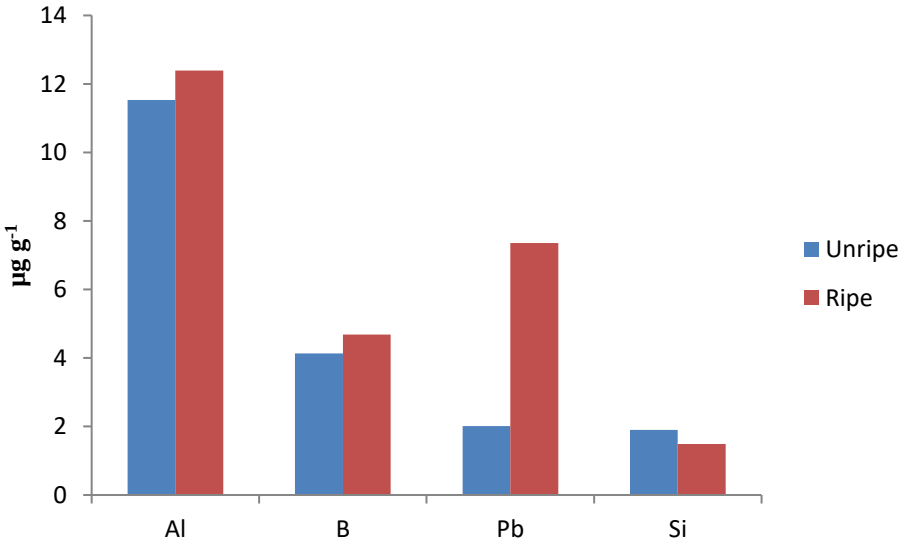

Figure 2. Content of Al, B, Pb and Si in analyzed *X. italicum* seed

Among elements presented in Figure 2, Al, B and Si have certain functions in plant tissues, in small amounts, whereas Pb is toxic to plant tissues.

Despite the abundance of aluminum (it is the third most abundant element after oxygen and silicon in the earth's crust), it is not considered as an essential element, and so far no experimental evidence has been put forward for a biological role. Its availability depends on soil pH. It is interesting that aluminum can have a beneficial or toxic effect, depending on different factors such

as the chemical form of Al, metal concentration, plant species, physiological age, the duration of exposure to the metal and growth conditions. Aluminum content varied from 11.5 to 12.4 μg/g, which is not a significant difference for unripe and ripe *X. italicum* seeds. Si and B content was lower compared to Al. Boron is an essential or at least highly beneficial micronutrient for animal organisms, affecting the metabolism of macro minerals Ca, P, and Mg, proteins, triglyceride, amino acids, glucose, steroid hormones, and reactive oxygen species. Plants take up boron in the form of small uncharged boric acid molecules, as well as borate anions (Brdar-Jokanović, 2020). Same as in the case of aluminum, boron content was lower in unripe (4.1 μg/g), compared to ripe (4.7 μg/g) seed, but this difference was not statistically significant.

Lead is an extremely toxic element and plants have no channels for its uptake, so it is unknown how exactly it enters the root. It can remain attached to the carboxyl groups of uronic acids on the root surface. Lead is mostly absorbed by the root and remains in it, thus making the root the first barrier for further transport of Pb to the aerial parts of the plant, where its phytotoxicity could be fatal. Its adverse effects on mineral nutrition, water content, photosynthesis, morphology, seed germination, seedling growth, and enzymatic activities are confirmed for all plant species. In higher concentrations lead inhibits root and leaf growth, photosynthesis, and affects the morphological and anatomical structure of plants. Analyzed *X. italicum* seed showed high concentrations of Pb, 2.0 and 7.4 μg/g for unripe and ripe fruit, respectively (Figure 2).

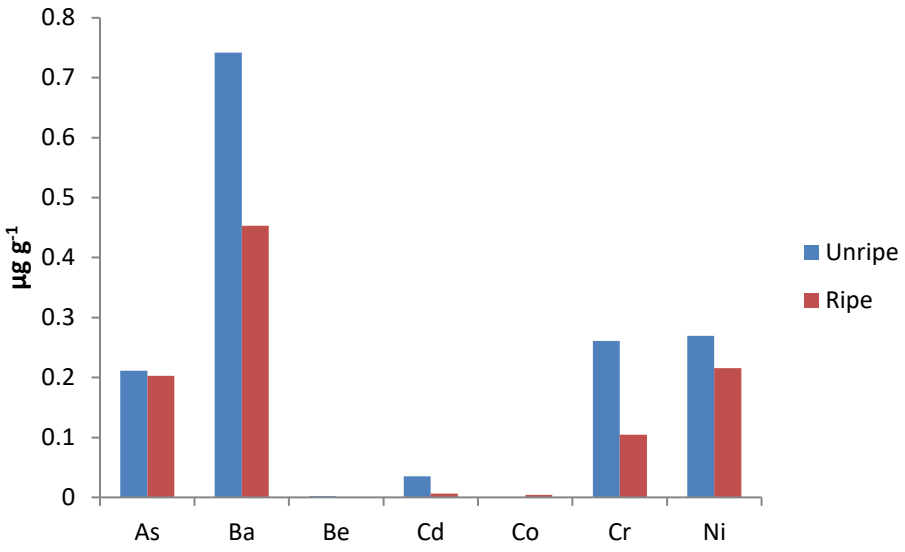

Figure 3. Content of As, Ba, Be, Cd, Co, Cr and Ni in analyzed *X. italicum* seed

According to WHO (1996) recommended permissible limit for Pb is 2 μg/g. The Pb level in the analyzed plant is higher than the permissible level, indicating that this plant could be used in Pb remediation from soil. The increased content of Pb can be explained by its presence in the soil, which originates from exhaust gases of motor vehicles, as well as from air transport and its deposition from air to soil and plant. Davies and Holmes (1972) found that if the content of Pb in gasoline is 0.45 g/L and if the flow rate of the vehicle is 24h, then on both sides road with a width of 15 m, with every 1000 vehicles, the concentration of lead in the air increases for 1 $\mu g/m^3$.

Arsenic is a non-essential and generally toxic element to plants, which inhibits root extension and proliferation, inhibits biomass production, interferes with metabolic processes and can severely inhibit plant growth by compromising plant reproductive capacity. As^{5+} is easily mobilized and taken up by plants through phosphate transport pathways. Due to their chemical similarity, As^{5+} competes with phosphates in the uptake process and it interferes with metabolic processes, such as the synthesis of ATP and oxidative phosphorylation. Arsenic can severely inhibit plant growth by compromising plant reproductive capacity. Arsenic content in unripe and ripe seeds did not vary significantly (0.21 μg/g and 0.20 μg/g, respectively) (Figure 3). According to FAO/WHO (1999) maximum permissible level for As in plants is 0.1 μg/g, which is twice lower than As content in *X. italicum* from this study. Since this plant is characterized as a honey plant, this could affect honey quality.

Chromium is an element classified as a carcinogen agent according to the International Agency for Research on Cancer. The toxic effects of Cr are correlated with the generation of reactive oxygen species (ROS), which cause oxidative stress in plants. The most common and stable states of chromium are hexavalent (Cr (VI)) and trivalent (Cr (III)) (IARC, 1987). Due to its high redox potential and intricate electronic and valence shell chemistry, chromium can easily convert from one oxidation state to another. Under physiological conditions, Cr (VI) enters the cells and may get reduced to Cr (V), Cr (IV), triradicals, hydroxyl radicals and finally Cr (III). All these oxidation states disrupt the cellular integrity of cells by attacking proteins, DNA and membrane lipids (Sharma et al., 2020). According to literature data, the concentration of chromium in plants is very low. The average chromium concentration in plant tissues is 0.2 to 4 mg/kg of dry plant matter. Cr excess in plants results in chlorosis and growth inhibition. Chromium concentration is twice higher in unripe (0.26 μg/g) compared to ripe seed (0.10 μg/g) in the presented study (Figure 3).

Compared to the maximum permissible level of Cr prescribed by FAO/WHO (1999) *X. italicum* from this study showed a 10 times lower concentration. Chirigiu et al. (2003) reported 5.525 μg g^{-1} of Cr in *X. italicum* and 0.562 μg g^{-1} in *X. spinosum*, so *X. italicum* from our study is more similar to *X. spinosum* by Cr content.

Same as Cr, nickel can also result in chlorosis in plant tissues in higher concentrations. Nickel helps plants to absorb Fe from the soil. It is very important for urease activity and has an impact on seed germination, too. Plants suffering from Ni deficiency show necrosis initiating from the tip of the leaf. Same as in the case of Cr, Ni concentration is higher in unripe (0.27 μg/g) compared to ripe (0.21 μg/g) seed (Figure 3).

Cadmium is an element with a very toxic effect on plants, animals, and humans. It is an extremely mobile element in the soil, easily transported through the plant and distributed to all plant organs subsequently. Cd and Zn are very similar, and in addition, Cd can imitate the behavior of some other essential elements in uptake from the soil and metabolism. The main cause of cadmium toxicity represents the high affinity of Cd for thiol groups in enzymes and proteins. Higher concentrations in plants inhibit iron metabolism and reduce the intensity of photosynthesis. The content of Cd (0.006 μg/g in ripe seed and 0.035 μg/g in unripe seed, Figure 3) is significantly lower compared to the WHO recommended value of 0.3 μg/g. It has been observed that high concentrations of Fe in the soil reduce Cd uptake by plants. Other metals, such as Zn, Ca, Mg and Cu, can also inhibit the uptake of Cd from the rhizosphere, among which the level of Ca has the strongest effect, as both these ions can pass through the membrane and via cation channels, their competition is very pronounced.

Conclusion

The content of 20 elements (Al, As, B, Ba, Be, Ca, Cd, Co, Cr, Cu, Fe, K, Mg, Mn, Na, Ni, P, Pb, Si, Zn) was determined in unripe and ripe *X. italicum* unripe and ripe seed. Out of the analyzed macroelements, K showed the highest concentrations in ripe and unripe seeds, while the lowest concentration was recorded for Na. Fe is the most abundant microelement, and it showed a five times higher concentration in unripe compared to a ripe seed. Surprisingly, Pb content was higher than WHO permissible limits, which might be because plant samples are collected near the road.

The content of Fe, Ba, Cr, Cu, Mn, Pb, and Zn differ in the ripe and unripe stages of the analyzed seed, which indices that elemental composition is affected by the vegetative stage.

Acknowledgment

The authors would like to thank the Ministry of Education, Science and Technological Development of Republic of Serbia (Grant No: 451-03-9/2021-14/200124 and 451-03-9/2022-14/200124) for financial support.

Conflict-of-Interest Statement

The authors did not declare any conflict of interest.

References

Anastasiu, P., Negrean, G., Basnou, C., Sîrbu, C., & Oprea, A. (2007). A preliminary study on the neophytes of wetlands in Romania. Neobiota, 7, 181-192.

Bai, Q., Shen, Y., & Huang, Y. (2021). Advances in mineral nutrition transport and signal transduction in Rosaceae fruit quality and postharvest storage. Frontiers in Plant Science, 12, 620018.

Baiyeri, K.P. (2000). Effect of nitrogen fertilization on mineral concentration in plantain (Musa AAB) fruit peel and pulp at unripe and ripe stages. Plant Products Research Journal, 5, 38-43.

Baiyeri, K.P., & Unadike, G.O. (2001). Ripening stages and days after harvest influenced some biochemical properties of two Nigerian plantain (Musa species AAB) cultivars. Plant Products Research Journal, 6, 11-19.

Brdar-Jokanović, M. (2020). Boron toxicity and deficiency in agricultural plants. International Journal of Molecular Sciences, 21, 1424.

Chirigiu, L., Tiţa, I., Radu, S., & Capitanescu, C. (2003). Content of metals in the seeds of *Xanthium spinosum* and *Xanthium italicum*. Fitoterapia, 74, 168-169.

Davies, B.E., & Holmes, P.L. (1972). Lead contamination of roadside soil and grass in Birmingham, England, in relation to naturally occurring levels. Journal of Agricultural Science, 79, 479-484.

Economou, G., Bilalis, D., & Avgoulas, C. (2005). Weed flora distribution in Greek cotton fields and its possible influence by herbicides. Phytoparasitica, 33, 406-419.

Fetvadjieva, N., & Milanova, S. (1998). Cocklebur advancing on our fields. Plant Protection, 5, 20-22.

Galanos, C.J. (2015). The alien flora of terrestrial and marine ecosystems of Rodos island (SE Aegean), Greece. Willdenowia, 45, 261-278.

IARC (1987). IARC monographs on the evaluation of the carcinogenic risks to humans. Overall evaluations of carcinogenicity: And updating of IARC monographs, volumes 1 to 42. IARC monographs Supplement 7, 1–440.

Ilić, O., & Nikolić, Lj. (2011). Ecological characteristics of ass. *Panico-galinsogetum* Tx. et Beck. 1942 in potato crop. Herbologia, 12, 77-88.

Imelouane, B., Tahri, M., Elbastrioui, M., Aouinti, F., & Elbachiri, A. (2011). Mineral contents of some medicinal and aromatic plants growing in eastern Morocco. Journal of Materials and Environmental Science, 2, 104-111.

Izonfuo, W.-A.L., & Omuaru, V.O.T. (1988). Effect of ripening on the chemical composition of plantain peels and pulps (*Musa paradisiaca*). Journal of the Science of Food and Agriculture, 45, 333-336.

Kabata-Pendias, A., & Pendias, H. (1992). Trace elements in soils and plants. (2nd ed.). Boca Raton: CRC Press Inc.

Manilov, T., & Zhalnov, I. (2018). Weed control in ExpresSun® sunflower (*Helianthus annuus* L.). Zbornik radova, 53. Hrvatski i 13. Međunarodni Simpozij Agronoma, Vodice, Hrvatska.

Mari, S., Bailly, C., & Thomine, S. (2020). Handing off iron to the next generation: how does it get into seeds and what for? Biochemical Journal, 477, 259–274.

Novák, R., Dancza, I., Szentey, L., & Karamán, J. (2009). Arable weeds of Hungary. Fifth National Weed Survey (2007-2008). Ministry of Agriculture and Rural Development, Budapest, Hungary.

Paul, V., Pandey, R., Ramesh, K.V., & Singh, A. (2012). Role of mineral nutrients in physiology, ripening and storability of fruits. Advances in Plant Physiology, 13, 56–96.

Ramirez-Erosa, I., Huang, Y., Hickie, R.A., Sutherland, R.G., & Barl, B. (2007). Xanthstin and xanthinosin from the burs of *Xanthium strumarium* L. as potential anticancer agents. Canadian Journal of Physiology and Pharmacology, 85, 1160-1172.

Shao, H., Huang, X., Wei, X., & Zhang, C. (2012). Phytotoxic effects and a phytotoxin from the invasive plant *Xanthium italicum* Moretti. Molecules, 17, 4037-4046.

Sharma, A., Kapoor, D., Wang, J., Shahzad, B., Kumar, V., Bali, A.S., Jasrotia, S., Zheng, B., Yuan, H., & Yan, D. (2020). Chromium bioaccumulation and its impacts on plants: An overview. Plants, 9, 100.

Stevanović, J., Stavretović, N., Obratov-Petković, D., & Mijović, A. (2009). Ivazivne biljne vrste na nekim sportsko-rekreativnim površinama Beograda. Acta Herbologica, 18, 115-125.

Trankner, M., Tavakol, E., & Jakli, B. (2018). Functioning of potassium and magnesium in photosynthesis, photosynthate translocation and photoprotection. Physiologia Plantarum, 163, 414–431.

US EPA (1996). Method 3050B: Acid Digestion of Sediments, Sludges and Soils.

Versieren, L., Evers, S., AbdElgawag, H., Asard, H., & Smolders, E. (2017). Mixture toxicity of copper, cadmium, and zinc to barley seedlings is not explained by antioxidant and oxidative stress biomarkers. Environmental Toxicology and Chemistry, 36, 220-230.

White, P. J., & Karley, A. J. (2010). Potassium Cell Biology of Metals and Nutrients. Berlin: Springer, 199–224.

WHO (1996). https://www.omicsonline.org/articles-images/2161-0525-5-334-t011.html

Wiedenhoeft, A.C. (2006). Plant Nutrition. (1st ed.). New York: Chelsea House Pub.

Yoou, J.H., Lim, H.J., Lee, H.J., Kim, H.-D., Jeon, R., & Ryu, J.-H. (2008). Inhibition of lipopolysaccharide-induced inducible nitric oxide synthase and cyclooxygenase-2 expression by xanthanolides isolated from *Xanthium strumarium*. Bioorganic & Medicinal Chemistry Letters, 18, 2179-2182.

Zima, D., & Štefanić, E. (2018). Analiza medonosnosti invazivnih biljnih vrsta Požeške kotline. Zbornik radova, 53. Hrvatski i 13. Međunarodni Simpozij Agronoma, Vodice, Hrvatska.

Zrelo i nezrelo seme *Xanthium italicum* – elementni sastav

Marija Ilić[1], Violeta Mitić[2], Jelena Nikolić[2], Marija Marković[2], Jelena Mrmošanin[2], Aleksandra Pavlović[2], Vesna Stankov Jovanović[2]

1-Veterinarski specijalistički institut, Dimitrija Tucovića 175, Niš, Srbija

2-Univerzitet u Nišu, Prirodno-matematički fakultet, Departman za hemiju, Višegradska 33, Niš, Srbija

SAŽETAK

Sadržaj elemenata u biljkama zavisi od različitih faktora, kao što su biljna vrsta, period branja, karakteristike zemljišta i uslovi u životnoj sredini. Cilj ovog rada je ispitati primenom ICP OES tehnike elementalni sastav zrelog i nezrelog semena biljne vrste *Xanthium italicum* sakupljenog u selu Temska. Element sa najvećom koncentracijom u analiziranim uzorcima je kalijum, čiji se sadržaj značajno razlikuje u zrelom i nezrelom semenu. Gvožđe ima pet puta veću koncentraciju u nezrelom (27.7 μg/g), u poređenju sa zrelim (6.2 μg/g) semenom. Sadržaj Ba, Cr, Cu, Mn, Pb i Zn se takođe razlikuje u zrelim i nezrelim uzorcima analiziranog semena, što ukazuje da na elementni sastav utiče vegetativni period u kom se biljka nalazi. Sadržaj Pb i As veći je od maksimalno dozvoljenih koncentracija, što može uticati na proizvodnju meda u ovom regionu, ako se u obzir uzme to da se ova biljna vrsta smatra medonosnom.

Ključne reči: Xanthium italicum, elementni sastav, ICP OES, seme

Graines mûres et non mûres de *Xanthium italicum* - composition élémentaire

Marija Ilić[1], Violeta Mitić[2], Jelena Nikolić[2], Marija Marković[2], Jelena Mrmošanin[2], Aleksandra Pavlović[2], Vesna Stankov Jovanović[2]

1- Institut vétérinaire spécialisé, Dimitrija Tucovića 175, Niš, Serbie

2- Université de Niš, Faculté des sciences naturelles et des mathématiques, Département de biologie et d'écologie, Višegradska 33, Niš, Serbie

RÉSUMÉ

La teneur des éléments dans les plantes dépend de divers facteurs, tels que les espèces végétales, la période de récolte, les caractéristiques du sol et les conditions environnementales. L'objectif de cette étude est d'examiner la composition élémentaire de graines mûres et non mûres de l'espèce végétale *Xanthium italicum* recueillies dans le village de Temska à l'aide de l'ICP OES. L'élément avec la plus grande concentration dans les échantillons analysés est le potassium, dont la teneur diffère significativement dans les graines mûres et non mûres. Le fer a une concentration cinq fois plus grande dans les graines non mûres (27,7 µg/g), que dans les graines mûres (6,2 µg/g). La teneur en Ba, Cr, Cu, Mn, Pb et Zn est également différente dans les échantillons mûrs et non mûrs des graines analysées, ce qui indique que la composition élémentaire est affectée par la période végétative dans laquelle se trouve la plante. La teneur en Pb et As est supérieure à la concentration maximale autorisée, ce qui peut influencer la production de miel dans cette région, si l'on prend en compte le fait que cette espèce végétale est considérée comme mellifère.

Mots-clés: Xanthium italicum, composition élémentaire, ICP OES, graines

Зрелые и незрелые семена *Xanthium italicum* - элементный состав

Мария Илич[1], Виолета Митич[2], Елена Николич[2], Мария Маркович[2], Елена Мрмошанин[2], Александра Павлович[2], Весна Станков Йованович[2]

1-Ветеринарный специализированный институт, Дмитрия Туковича 175, Ниш, Сербия

2-Нишский университет, Естественно-математический факультет, кафедра химии, Вышеградская 33, Ниш, Сербия

Резюме

Содержание элементов в растениях зависит от различных факторов, таких как вид растений, период сбора урожая, характеристики земли и условий окружающей среды. Целью данной работы является изучение элементного состава зрелых и незрелых семян видов растений *Xanthium italicum*, собранных в селе Темска с использованием метода ICP OES. Элемент с наибольшей концентрацией в анализируемых образцах - калий, содержание которого значительно различается в зрелых и незрелых семенах. Железо имеет в пять раз более высокую концентрацию в незрелом (27, 7 мкг/г), по сравнению со зрелым (6, 2 мкг/г) семенем. Содержание Ba, Cr, Cu, Mn, Pb и Zn также различается в зрелых и незрелых образцах анализируемых семян, что указывает на то, что на элементный состав влияет вегетативный период, в котором находится растение. Содержание Pb и As выше максимально допустимых концентраций, что может повлиять на производство меда в этом регионе, если учесть, что этот вид растений считается медоносным.

Ключевые слова: Xanthium italicum, элементный состав, ICP OES, семена

Reife und unreife Samen von Xanthium italicum - Elementzusammensetzung

Marija Ilić[1], Violeta Mitić[2], Jelena Nikolić[2], Marija Marković[2], Jelena Mrmošanin[2], Aleksandra Pavlović[2], Vesna Stankov Jovanović[2]

1-Veterinärinstitut, Dimitrija Tucovića 175, Niš, Serbien

2-Universität Niš, Mathematisch-Naturwissenschaftliche Fakultät, Abteilung für Chemie, Višegradska 33, Niš, Serbien

ABSTRAKT

Der Gehalt an Elementen in Pflanzen hängt von verschiedenen Faktoren ab, wie beispielsweise Pflanzenart, Erntezeitpunkt, Bodeneigenschaften und Umweltbedingungen. Das Ziel dieser Arbeit ist die Untersuchung der Elementzusammensetzung von reifen und unreifen Samen der Pflanzenart *Xanthium italicum*, die im Dorf Temska unter Verwendung der ICP OES-Technik gesammelt wurden. Das Element mit der höchsten Konzentration in den analysierten Proben ist Kalium, dessen Gehalt sich in reifen und unreifen Samen deutlich unterscheidet. Eisen hat eine fünfmal höhere Konzentration (27,7 µg/g) in unreifen im Vergleich zu reifen Samen (6,2 µg/g). Der Gehalt an Ba, Cr, Cu, Mn, Pb und Zn unterscheidet sich ebenfalls in reifen und unreifen Proben des analysierten Samens, was darauf hinweist, dass die vegetative Phase, in der sich die Pflanze befindet, die Elementzusammensetzung beeinflusst. Der Gehalt an Pb und As überschreitet die zulässigen Höchstkonzentrationen, was sich auf die Honigproduktion in dieser Region auswirken kann, wenn man berücksichtigt, dass diese Pflanzenart als nektarliefernd gilt.

Schlüsselwörter: Xanthium italicum, elementare Zusammensetzung, ICP OES, Samen

Uptake of some heavy metal(oid)s by sunflower

Stefan Petrović[1*], Jelena Mrmošanin[1], Biljana Arsić[1], Aleksandra Pavlović[1], Snežana Tošić

1-University of Niš, Faculty of Sciences and Mathematics, Department of Chemistry, Višegradska 33, 18000 Niš, Republic of Serbia

ABSTRACT

Plant parts of sunflower (*Helianthus annuus* L.): root, stem, leaf, and seed, as well as the soil on which this plant culture was grown were analyzed for the content of As, Cd, Co, Cr, Cu, Fe, Mn, Ni, Pb, and Zn using Optical emission spectrometry with inductively coupled plasma (ICP-OES). The samples were prepared by wet digestion. To assess the degree of bioaccumulation in plant parts and the translocation of the examined elements from the roots to the above-ground plant parts, the Biological Concentration Factor (BCF), Mobility Ratio (MR), and Translocation Factor (TF) were calculated. BCF and MR values are less than 1 for all elements while TF (*leaf/root*) values for As, Cd, Cu, Fe, and Mn and TF (*stem/root*) values for Cu are higher than 1.

Keywords: sunflower, soil, heavy metal(oid)s, ICP-OES, bioaccumulation, translocation

[*] Corresponding author: stefan.petrovic@pmf.edu.rs

Introduction

Heavy metal(oid)s are considered to be the most common pollutants of the environment and their increased presence is a consequence of anthropogenic activities, such as mining (melting and galvanization of heavy metals), industrial waste, sewage sludge, exhaust emissions from vehicles, as well as agricultural activities: application of phosphate fertilizers, manure, and pesticides (Rai et al., 2019; Rezaeian et al., 2020; Sheoran et al., 2016).

A group of researchers from China conducted research with four commercial oil crops (rapeseed, sunflower, peanut, and sesame seeds) to use these agricultural species in the process of phytoremediation of agricultural soil contaminated with cadmium and lead due to mining activities. In a one-year field experiment, they applied three, so-called rotation systems (after harvesting the oilseed rape, sunflower, peanut, and sesame were planted separately and then harvested). In this experiment, 458.6 g/ha of Cd and 1264.7 g/ha of Pb were extracted by dry biomass in an oilseed rape-sunflower rotation system (Yang et al., 2017).

Liang et al. (2011) determined the content of Cd, Cr, and Pb in parts of sunflower (root, stem, leaf, and seed) as well as in the soil where sunflower was grown. This research showed that the use of wastewater for irrigation increased the heavy metal concentration in soil and plants.

Since sewage sludge is one of the potential pollutants of agricultural soil with heavy metals, Chen et al. (2010) provided a health risk assessment of heavy metals (Cd, Cr, Cu, Ni, Pb, and Zn) in maize, sunflower, and cotton seeds grown in China. These authors used High-Resolution Inductively Coupled Plasma Mass Spectrometry (HR-ICP-MS) to determine the content of heavy metals in the seeds of these crops. Sunflower seeds had the highest content of all tested metals.

Nehnevajova et al. (2005) examined the influence of fertilizers (ammonium sulfate and ammonium nitrate) on the uptake of Zn, Cd, and Pb by 15 varieties of sunflower using Flame Atomic Absorption Spectrometry (FAAS). They observed that sulfate improved the extraction of Zn and Pb while nitrate was most effective for Cd.

The aim of this work is to determine the content of As, Cd, Co, Cr, Cu, Fe, Mn, Ni, Pb, and Zn in the root, stem, leaf, and seed of sunflower, as well as in the soil on which this crop was grown, using Optical emission spectrometry with inductively coupled plasma (ICP-OES).

Experimental

The soil and plant material of sunflowers were sampled from an agricultural field in Deliblato Sand of the Republic of Serbia during the harvest of sunflowers in the autumn (September 2021) (Figure 1). Sampling was carried out from five different places along the diagonal of the field. Representative homogeneous samples from these soil and plant material subsamples were made.

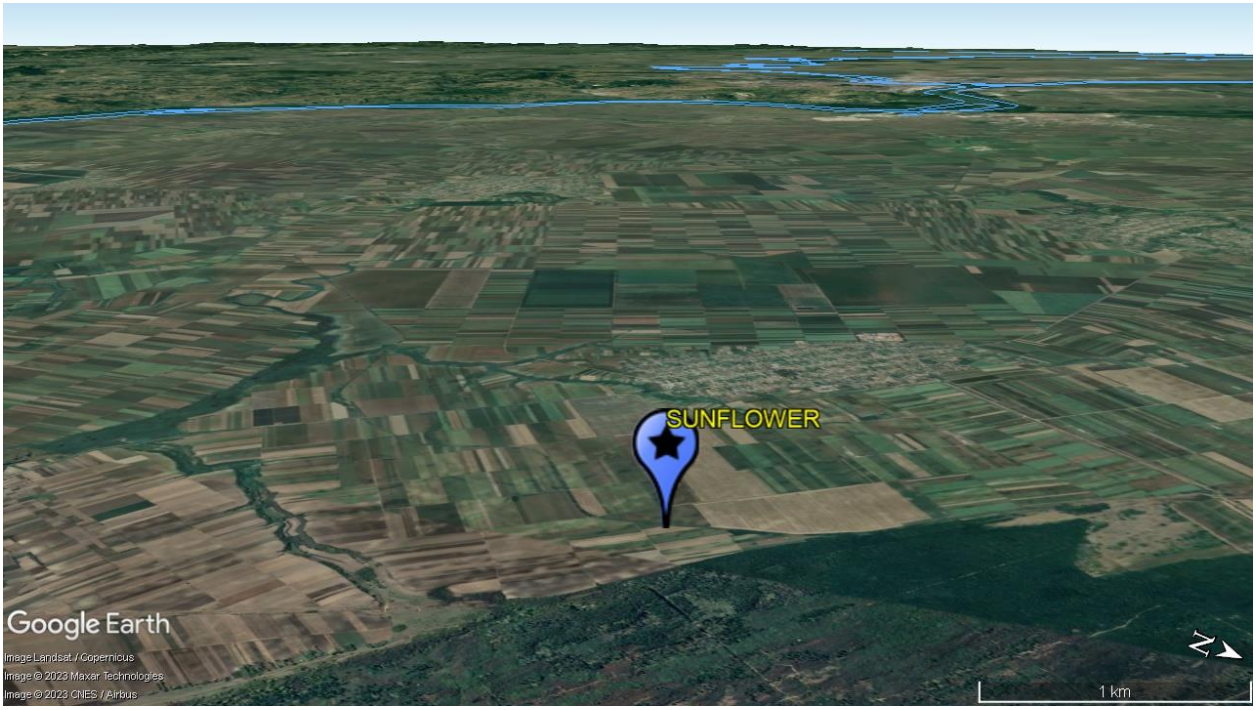

Figure 1. Agricultural field from which the soil and plant materials were sampled

Plant parts were divided into subsamples: root, stem, leaf, and seed. Sunflower roots were washed first with tap water and then deionized water, while the above-ground parts were analyzed unwashed. All plant material was air-dried for about 15 days, ground in a blender, and dried in the dryer at 65 °C for 8 hours.

The soil was air-dried for about 15 days, sifted through a sieve (2 mm diameter), and dried at 95 °C for 8 hours.

Preparation of soil sample for ICP-OES analysis

About 1 g of dry soil sample was measured into 100 mL conical flasks and 16 mL of *aqua regia* was added (mixture of conc. HNO_3 (Macron) and conc. HCl (Sigma-Aldrich), in a ratio 1:3, v/v) and left for about half an hour at room temperature. The contents were heated in a sandy bath

for an hour at about 190 °C almost to dryness, cooled to room temperature, and 6 mL of conc. H_2O_2 (Sigma-Aldrich) was added. The contents were reheated to a smaller volume. After cooling, 5 mL of deionized water was added. The contents were filtered through the filter paper (blue tape), and the filtrate was collected into 25 mL volumetric flasks and filled up to the mark with deionized water (Addis & Abebaw, 2017).

Preparation of plant material for ICP-OES analysis

About 1 g of sunflower root, stem, leaf, and seed samples were weighted into 100 mL conical flasks and 15 mL of conc. HNO_3 was added, and the contents were left at room temperature for about 30 minutes. The samples were then heated almost to dryness on a hot plate for about 1 hour. 5 mL conc. H_2O_2 was added to the cooled samples, evaporated again, and after cooling, 5 mL of deionized water was added to each conical flask. The samples were filtered through the filter paper (blue tape), and the filtrates were collected into 25 mL volumetric flasks and filled up to the mark with deionized water (Bargagli et al., 2000).

Parameters of ICP-OES instrument and characteristics of the calibration curve

The contents of the tested elements in soil and plant material samples were determined by the ICP-OES technique (iCAP 6000 series, ThermoScientific, Cambridge, United Kingdom) at the following optimal instrument parameters: flush pump rate-100 rpm, analysis pump rate-50 rpm, RF power-1150 W, nebulizer gas flow-0.7 L/min, coolant gas flow-12 L/min, auxiliary gas flow-0.5 L/min, plasma view-axial, washing time-30 s.

Multielement certified standard solution IV (Al, As, Ba, Be, B, Cd, Cr, Co, Cu, Fe, Pb, Mn, Ni, Se, Tl, V, and Zn; TraceCERT, Fluka Analytical, Switzerland) was used.The correlation coefficient (r), the limit of detection (LOD), and the limit of quantification (LOQ) of the working calibration curve for each tested element are shown in Table 1.

Table 1. The correlation coefficient (r), the limit of detection (LOD), and the limit of quantification (LOQ) of the calibration curve for each tested element

Element/ λ (nm)	r	LOD (ppm)	LOQ (ppm)	Element/ λ (nm)	r	LOD (ppm)	LOQ (ppm)
As 189.042	0.99993	0.00281	0.00936	**Fe 259.940**	0.99992	0.00052	0.00174
Cd 226.502	0.99985	0.00018	0.00061	**Mn 257.610**	0.99988	0.00012	0.00039
Co 228.616	0.9999	0.00029	0.00095	**Ni 231.604**	0.99989	0.00044	0.00146
Cr 267.716	0.99976	0.00063	0.00211	**Pb 220.353**	0.99993	0.00184	0.00613
Cu 324.754	0.99989	0.00062	0.00205	**Zn 202.548**	0.99977	0.00012	0.00029

Assessment of the bioaccumulation and transfer of tested elements

The degree of bioaccumulation of the studied elements in plant parts of sunflower is shown by bioaccumulation factors (BAFs) through the *Biological Concentration Factor* (BCF)-the ratio of metal(oid) concentration in the root and the concentration in the soil and *Mobility Ratio* (MR)-the ratio of metal(oid) concentration in the above-ground plant part and the concentration in the soil. The distribution of elements from the root to the above-ground parts of the sunflower is shown *via Translocation Factor* (TF)-the ratio of metal(oid) concentration in the above-ground plant part and the concentration in the root (Alagić et al., 2015; Antoniadis et al., 2017; Dimitrijević et al., 2016; Rai et al., 2019; Retamal-Salgado et al., 2017; Tošić et al., 2016).

Results and Discussion

The content of elements in soil samples and sunflower parts

The content of the studied elements in the plant parts of sunflowers, as well as in the soil on which this agricultural crop was grown are listed in Table 2. The most abundant element in the soil sample is Fe (7300 mg/kg) while the least abundant is Cd (1.12 mg/kg). None of the tested elements exceeds the maximum allowable concentration (MAC value) in the soil sample so the soil can be considered uncontaminated ("Official Gazette of the RS", No. 23/94, 1994).

The order of occurrence of the examined elements in the plant parts is quite uniform. The most abundant are Fe, Mn, Zn, and Cu, and the least abundant are Cd, As, and Co. It is interesting that the highest concentrations of essential metals Cu and Zn are in the seed; the largest part of Co, Cr, Ni, and Pb are retained in the roots, and the highest concentrations of Cd, Fe, and Mn are in the leaf. Concentrations of As, Cd, Co, Mn, Ni, Pb, and Zn in all plant parts are within normal concentrations in plant tissue. Chromium and iron concentrations in roots and leaves are, according to some studies, above normal concentrations, but certainly below phytotoxic values. The Cu content in the seeds is at the upper limit of normal concentrations in plant tissue (Alloway, 2013; Kabata-Pendias & Pendias, 2001; Nagajyoti et al., 2010; Vamerali et al., 2010) (Table 3).

In many published papers, the influence of different fertilizers on the uptake of some elements, as well as the influence of different pollutants, has been reported. Mineral fertilizers increase the bioavailability of microelements. Nehnevajova et al. (2005) examined the effect of sulfate and nitrate fertilizers on some microelements' adoption. Although the concentration of Cd in the soil in this paper is slightly higher (1.12 mg/kg) than the concentration in the work of

Nehnevajova et al. (2005) (0.9 mg/kg), the Cd concentrations are several times higher in the plant shoots grown in the presence of the mentioned fertilizers.

Liang et al. (2011) analyzed agricultural soil which was continuously contaminated with wastewater for at least 20 years through irrigation of agricultural crops grown on it. The concentrations of Cr and Pb were approximately two times higher than the concentration of these metals in the soil that was the subject of this study. Also, concentrations of these elements in sunflower stems and seeds are also approximately two times higher than the concentrations of these metals in sunflower parts in this paper. Thus, it can be concluded that sunflower has certain uptake abilities towards Pb and Cr.

The contents of Pb and Cd in the soil analyzed by Yang et al. (2017) are several times higher (Pb - about 40 times and Cd - about 9 times) than the contents of these metals in the soil analyzed in this paper. Also, concentrations of these heavy metals in the root, stem, leaf, and sunflower seeds are many times higher (even 700 times for Cd in the stem) than the concentrations in this paper, which is expected considering the degree of pollution of agricultural soil located near the mining district in southern China. This is just another confirmation that sunflower has a great affinity for Pb and Cd.

Table 2. The content of elements in the soil and parts of sunflower
(mean value ±SD, mg/kg dry matter)

El.	Soil	MAC (mg/kg)	Root	Stem	Leaf	Seed
As	6.693±0.008	25*	0.48±0.02	n.d.	0.49±0.03	n.d.
Cd	1.12±0.02	3*	0.1024±0.0000	0.0175±0.0000	0.140±0.003	0.082±0.003
Co	9.7±0.2	/	1.01±0.02	0.090±0.005	0.95±0.05	0.055±0.003
Cr	12.8±0.4	100*	4.74±0.09	0.30±0.02	4.3±0.2	0.25±0.02
Cu	19.8±0.3	100*	3.38±0.06	3.8±0.1	6.7±0.2	14.3±0.6
Fe	7300±100	/	770±10	50±2	890±40	33±2
Mn	294±4	1500-3000**	25.0±0.5	6.6±0.2	113±4	10.9±0.4
Ni	27.0±0.2	50*	4.87±0.04	0.45±0.02	4.3±0.2	1.30±0.01
Pb	17.4±0.3	100*	2.35±0.04	0.29±0.02	1.25±0.03	0.20±0.02
Zn	37.1±0.2	300*	9.62±0.03	4.50±0.04	8.3±0.2	22.7±0.2

* "Official Gazette of the RS", No. 23/94, (1994)

** Kabata-Pendias (2011)

n.d. – not detected

Chen et al. (2010) determined the contents of some heavy metals in sunflower seeds grown on soil contaminated with sewage sludge. The concentrations of Cd, Cu, Zn, Ni, and Pb were 2-3 times higher while the concentration of Cr was almost 20 times higher than the concentrations in this paper. The largest difference for Cr is most likely due to the high content of Cr in the soil (173.30 mg/kg).

Table 3. Normal concentrations and toxicity thresholds for the investigated metal(oid)s in plant tissue (mg/kg dry matter)

Element	Normal concentration	Toxicity threshold	Element	Normal concentration	Toxicity threshold
As	0.02-7[a]	5[c]	**Fe**	140[a]	/
Cd	0.1-2.4[a,b]	5-10[c] 10-20[d] 5-30[b]	**Mn**	15-100[a]	170-2000[c] 300-500[b]
Co	0.1-10[b]	/	**Ni**	1[a] 0.02-5[b]	20-30[c] 10-100[b]
Cr	0.2-1[a] 0.03-14[b]	5-30[b]	**Pb**	1-13[a] 0.1-10[d]	10-20[c] 30-300[b]
Cu	4-15[a,b]	5-40[b] for leaf 100-400[b] for root	**Zn**	8-100[a]	150-200[c,d] 100-500[b]

[a]Nagajyoti et al. (2010), [b]Alloway (2013), [c]Vamerali et al. (2010), [d]Kabata-Pendias & Pendias (2001)

Assessment of the bioaccumulation capacity of sunflower according to the tested elements

The ability of the sunflower to accumulate the tested elements in the root was assessed using the BCF values shown in Figure 2.

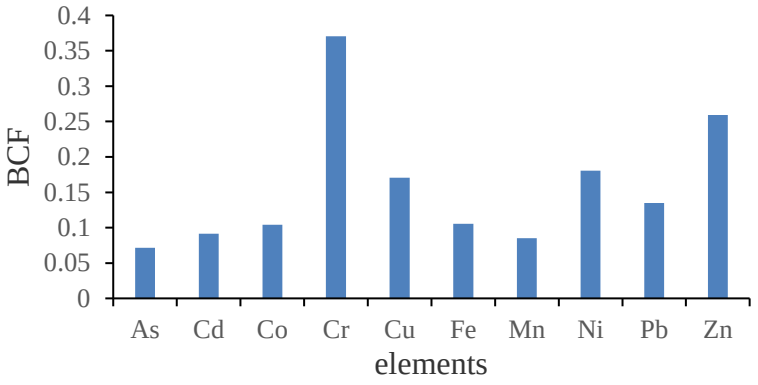

Figure 2. BCF values for sunflower root

The bioaccumulation ability of sunflower root according to the tested elements grows in the sequence As<Mn<Cd<Co<Fe<Pb<Cu<Ni<Zn<Cr. The BCF values are quite less than 1, which indicates a low accumulation of these metals in sunflower roots. Chromium is the metal that the sunflower plant deposits mostly in the root. Yang et al. (2017) have shown in their field experiment that the BCF values for Pb were very low while those values for Cd were higher than 1 in all plant parts except seed. Liang et al. (2011) calculated the BCF values for sunflower root for Cr, Pb, and Cd and according to their results, the highest BCF value was reported for Cr.

Assessment of the uptake of studied elements by above-ground parts of sunflower from the soil

Figure 3 shows a histogram with the MR values for the sunflower stem and leaf. Obtained values are less than 1, which means that the contents of the elements in the stem and leaf are less than the contents in the soil. The MR factor for *leaf/soil* is higher than the *stem/soil* factor for all elements. Yang et al. (2017) reported that the MR values (*leaf/soil*) for Cd and Pb are also higher than the MR (*stem/soil*) values. Liang et al. (2011) showed that the MR (*stem/soil*) for sunflowers follows the next order: Cd<Pb<Cr which is consistent with the results in this study.

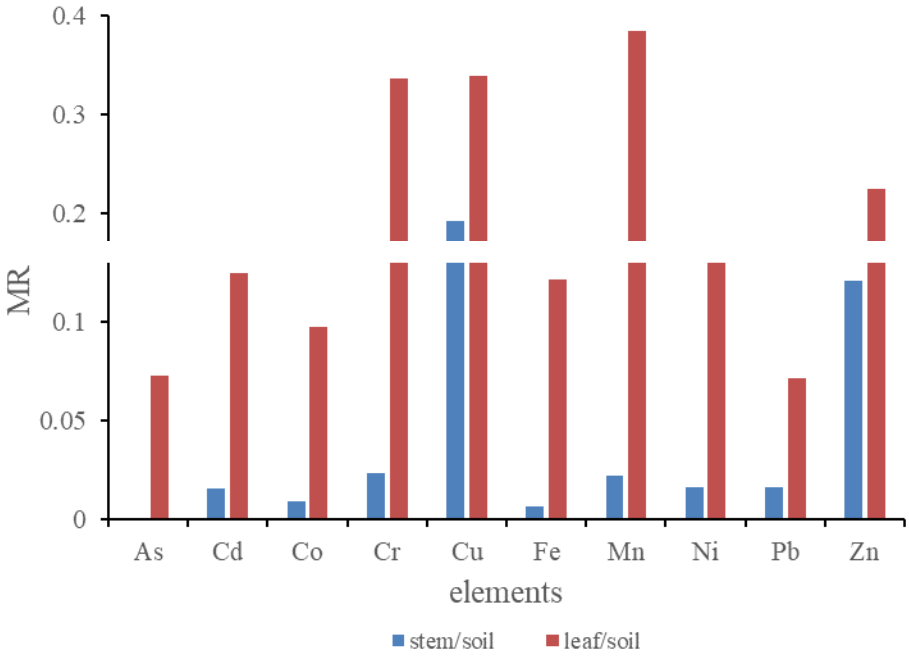

Figure 3. MR values for sunflower parts

Assessment of the distribution of tested elements from the roots to the above-ground parts of the sunflower

In general, the TF (*leaf/root*) values are higher than the TF (*stem/root*) values for all elements (Figure 4). The TF factors for *leaf/root* are higher than 1 for As, Cd, Cu, Fe, and Mn while TF is higher than 1 for *stem/root* for Cu only. The highest TF values are for Mn and Cu, 4.52 and 1.98 respectively. Copper and manganese are cofactors of the enzymes Cu/Zn-SOD and Mn-SOD (superoxide dismutase, SOD), and their significant role in the antioxidant system of the plant is directly related to the significant translocation of these metals in the above-ground parts of sunflower. Iron is slightly less common in superoxide dismutase (Fe-SOD), but it is present in redox enzymes (Fe-S proteins), which is also related to the noticeable transfer of this metal from the root to the leaf (Nagajyoti et al., 2010).

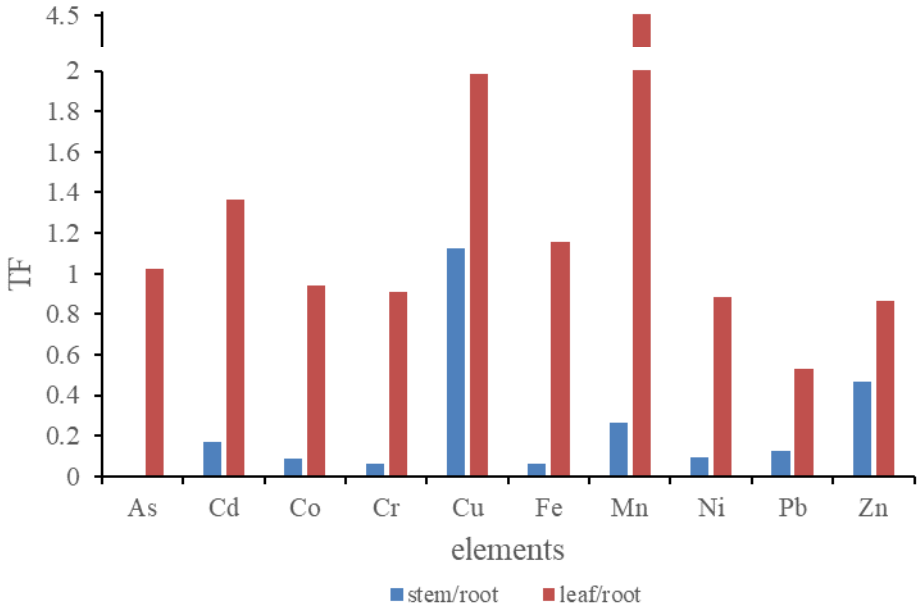

Figure 4. TF values for sunflower parts

Conclusion

The most abundant elements in soil and plant parts of sunflowers are Fe, Mn, Zn, and Cu, and the Cd, As, and Co are the least abundant. All soil concentrations are below the MAC values, and plant parts concentrations are within normal concentrations or at the upper limit of normal concentrations in plant tissue but certainly below phytotoxic values. The order of presence of the

examined elements in the studied parts of the plant is different for different metal(oid)s. The calculated factors show that Cr is mostly deposited in the roots as well as MR (*leaf/soil)* and TF (*leaf/root)* are higher than the corresponding values for the *stem/soil* and *stem/root* systems for all elements which is probably a consequence of the specificity of the plant species itself as well as potential foliar uptake. A good translocation from the root to the leaf was observed for As, Cd, Cu, Fe, and Mn and to the stem for Cu.

Acknowledgment

The research was supported by the Ministry of Education, Science and Technological Development of the Republic of Serbia (Projects No. 451-03-47/2023-01/ 200124).

Conflict-of-Interest Statement

None.

References

Addis, W., & Abebaw, A. (2017). Determination of heavy metal concentration in soils used for cultivation of *Allium sativum* L. (garlic) in East Gojjam Zone, Amhara Region, Ethiopia. Cogent Chemistry, 3(1), 1–12. doi: 10.1080/23312009.2017.1419422

Alagić, S. Č., Tošić, S. B., Dimitrijević, M. D., Antonijević, M. M., & Nujkić, M. M. (2015). Assessment of the quality of polluted areas based on the content of heavy metals in different organs of the grapevine (*Vitis vinifera*) cv Tamjanika. Environmental Science and Pollution Research, 22(9), 7155–7175. doi: 10.1007/s11356-014-3933-1

Alloway, B. J. (2013). Heavy metals in soils (3rd ed.). London: Springer.

Antoniadis, V., Levizou, E., Shaheen, S. M., Ok, Y. S., Sebastian, A., Baum, C., Prasad, M. N. V., Wenzel, W. W., & Rinklebe, J. (2017). Trace elements in the soil-plant interface: Phytoavailability, translocation, and phytoremediation–A review. Earth-Science Reviews, 171, 621–645. doi: 10.1016/j.earscirev.2017.06.005

Bargagli, R., Borghini, F., & Celesti, C. (2000). Elemental composition of the lichen *Umbilicaria decussata*. Italian Journal of Zoology, 67(1), 157–162. doi: 10.1080/11250000009356371

Chen, Z.-F., Zhao, Y., Zhu, Y., Yang, X., Qiao, J., Tian, Q., & Zhang, Q. (2010). Health risks of heavy metals in sewage-irrigated soils and edible seeds in Langfang of Hebei province, China. Journal of the Science of Food and Agriculture, 90(2), 314–320. doi: 10.1002/jsfa.3817

Dimitrijević, M. D., Nujkić, M. M., Alagić, S. Č., Milić, S. M., & Tošić, S. B. (2016). Heavy metal contamination of topsoil and parts of peach-tree growing at different distances from a smelting complex. International Journal of Environmental Science and Technology, 13(2), 615–630. doi: 10.1007/s13762-015-0905-z

Kabata-Pendias, A. (2011). Trace elements in soils and plants (4th ed.). CRC Press.

Kabata-Pendias, A., & Pendias, H. (2001). Trace elements in soils and plants (3rd ed.). Boca Raton: London, New York, Washington.

Liang, J., Chen, C., Song, X., Han, Y., & Liang, Z. (2011). Assessment of heavy metal pollution in soil and plants from Dunhua sewage irrigation area. International Journal of Electrochemical Science, 6(11), 5314–5324.

Nagajyoti, P. C., Lee, K. D., & Sreekanth, T. V. M. (2010). Heavy metals, occurrence and toxicity for plants: a review. Environmental Chemistry Letters, 8(3), 199–216. doi: 10.1007/s10311-010-0297-8

Nehnevajova, E., Herzig, R., Federer, G., Erismann, K.-H., & Schwitzguébel, J.-P. (2005). Screening of sunflower cultivars for metal phytoextraction in a contaminated field prior to mutagenesis. International Journal of Phytoremediation, 7(4), 337–349. doi: 10.1080/16226510500327210

"Official Gazette of the RS", No. 23/94 (1994). Rulebook on allowable quantities of dangerous and hazardous matters in soil and irrigation water and methods for their testing.

Rai, P. K., Lee, S. S., Zhang, M., Tsang, Y. F., & Kim, K.-H. (2019). Heavy metals in food crops:

Health risks, fate, mechanisms, and management. Environment International, 125, 365–385. doi: 10.1016/j.envint.2019.01.067

Retamal-Salgado, J., Hirzel, J., Walter, I., & Matus, I. (2017). Bioabsorption and bioaccumulation of cadmium in the straw and grain of maize (Zea mays L.) in growing soils contaminated with cadmium in different environment. International Journal of Environmental Research and Public Health, 14(11), 1–15. doi: 10.3390/ijerph14111399

Rezaeian, M., Moghadam, M. T., Kiaei, M. M., & Zadeh, H. M. (2020). The effect of heavy metals on the nutritional value of alfalfa: comparison of nutrients and heavy metals of alfalfa (*Medicago sativa*) in industrial and non-industrial areas. Toxicological Research, 36(2), 183–193. doi: 10.1007/s43188-019-00012-6

Sheoran, V., Sheoran, A. S., & Poonia, P. (2016). Factors affecting phytoextraction: A review. Pedosphere, 26(2), 148–166. https://doi.org/10.1016/S1002-0160(15)60032-7

Tošić, S., Alagić, S., Dimitrijević, M., Pavlović, A., & Nujkić, M. (2016). Plant parts of the apple tree (*Malus* spp.) as possible indicators of heavy metal pollution. Ambio, 45(4), 501–512. doi: 10.1007/s13280-015-0742-9

Vamerali, T., Bandiera, M., & Mosca, G. (2010). Field crops for phytoremediation of metal-contaminated land. A review. Environmental Chemistry Letters, 8(1), 1–17. doi: 10.1007/s10311-009-0268-0

Yang, Y., Zhou, X., Tie, B., Peng, L., Li, H., Wang, K., & Zeng, Q. (2017). Comparison of three types of oil crop rotation systems for effective use and remediation of heavy metal contaminated agricultural soil. Chemosphere, 188, 148–156. doi: 10.1016/j.chemosphere.2017.08.140

Usvajanje nekih teških metal(oid)a od strane suncokreta

Stefan Petrović[1], Jelena Mrmošanin[1], Biljana Arsić[1], Aleksandra Pavlović[1], Snežana Tošić[1]

1-Univerzitet u Nišu, Prirodno-matematički fakultet, Departman za hemiju, Višegradska 33, 18000 Niš, Republika Srbija

SAŽETAK

Biljni delovi suncokreta (*Helianthus annuus* L.): koren, stabljika, list i seme, kao i zemljište na kome je uzgajana ova biljna kultura analizirani su na sadržaj As, Cd, Co, Cr, Cu, Fe, Mn, Ni, Pb i Zn primenom optičke emisione spektrometrije sa induktivno spregnutom plazmom (*engl.* ICP-OES). Uzorci su pripremljeni postupkom mokre digestije. Za procenu stepena bioakumulacije u biljnim delovima i translokacije ispitivanih elemenata iz korena u nadzemne delove biljke, izračunate su BCF (*engl. Biological concentration factor*), MR (*engl. Mobility ratio*) i TF (*engl. Translocation factor*) vrednosti. BCF i MR vrednosti su manje od 1 za sve ispitivane elemente dok su TF vrednosti (*list/koren*) za As, Cd, Cu, Fe i Mn kao i TF vrednost (*stabljika/koren*) za Cu veće od 1.

Ključne reči: suncokret, zemljište, teški metal(oid)i, ICP-OES, bioakumulacija, translokacija

Absorption de certains métaux et métalloïdes lourds par le tournesol

Stefan Petrović[1], Jelena Mrmošanin[1], Biljana Arsić[1], Aleksandra Pavlović[1], Snežana Tošić[1]

1- Université de Niš, Faculté des sciences naturelles et des mathématiques, Département de chimie, Višegradska 33, 18000 Niš, Serbie

RÉSUMÉ

Les parties végétales du tournesol (*Helianthus annuus* L.): racine, tige, feuille et graine, ainsi que le sol sur lequel cette culture végétale a été cultivée ont été analysés pour la teneur en As, Cd, Co, Cr, Cu, Fe, Mn, Ni, Pb et Zn en utilisant la spectrométrie d'émission optique avec plasma à couplage inductif (ICP-OES). Les échantillons ont été préparés par digestion humide. Pour évaluer le degré de bioaccumulation dans les parties de la plante et la translocation des éléments examinés des racines vers les parties aériennes de la plante, le facteur de bioconcentration (FBC), le rapport de mobilité (RM) et le facteur de translocation (TF) ont été calculés. Les valeurs BCF et MR sont inférieures à 1 pour tous les éléments, tandis que les valeurs TF (feuille/racine) pour As, Cd, Cu, Fe et Mn et la valeur TF (tige/racine) pour Cu est supérieure à 1.

Mots-clés: tournesol, sol, métaux et métalloïdes lourds, ICP-OES, bioaccumulation, translocation

Усвоение некоторых тяжелых металлов (металлоидов) подсолнухами

Стефан Петрович[1], Елена Мрмошанин[1], Биляна Арсич[1], Александра Павлович[1], Снежана Тошич[1]

1-Нишский университет , Естественно-математический факультет , кафедра химии, Вышеградская 33, Ниш, Сербия

Резюме

Растения подсолнечника (*Helianthus annuus* L.) корень, стебель, лист и семена, а также землю, на которой выращивали эту растительную культуру, анализировали на содержание As, Cd, Co, Cr, Cu, Fe, Mn, Ni, Pb и Zn с помощью индуктивно связанной плазменной оптической эмиссионной спектрометрии (англ. ICP-OES). Образцы готовили методом влажной дигестии. Для оценки степени биоаккумуляции в частях растений и транслокации исследуемых элементов из корней в надземные части растений были рассчитаны BCF (англ. *Biological concentration factor*), MR (*англ. Mobility ratio*) и TF (*англ. Translocation factor*). Значения BCF и MR меньше 1 для всех исследуемых элементов, тогда как значения TF (list/корень) для As, Cd, Cu, Fe и Mn, а также значения TF (корень/корень) для Cu больше 1.

Ключевые слова: подсолнечник, земля, тяжелый металл (oid)i, ICP-OES, биоаккумуляция, транслокация

Aufnahme einiger Schwermetallen durch Sonnenblumen

Stefan Petrović[1], Jelena Mrmošanin[1], Biljana Arsić[1], Aleksandra Pavlović[1], Snežana Tošić[1]

1- Universität Niš, Mathematisch-Naturwissenschaftliche Fakultät, Abteilung für Chemie, Višegradska 33, 18000 Niš, Republik Serbien

ABSTRAKT

Pflanzenteile der Sonnenblume (*Helianthus annuus* L.): Wurzel, Stängel, Blätter und Samen sowie der Boden, auf dem diese Pflanzenkultur angebaut wurde, wurden mittels optischer Emissionsspektrometrie mit induktiv gekoppeltem Plasma (ICP-OES) auf den Gehalt an As, Cd, Co, Cr, Cu, Fe, Mn, Ni, Pb und Zn analysiert. Die Proben wurden mittels Nassaufschlussverfahren vorbereitet. Um den Grad der Bioakkumulation in Pflanzenteilen und die Translokation der untersuchten Elemente von den Wurzeln zu den oberirdischen Pflanzenteilen zu beurteilen, wurden die Werte für den biologischen Konzentrationsfaktor (BCF, engl. *Biological concentration factor*), das Mobilitätsverhältnis (MR, engl. *Mobility ratio*) und den Translokationsfaktor (TF, engl. Translocation factor) berechnet. Die BCF- und MR-Werte sind für alle untersuchten Elemente kleiner als 1, während die TF-Werte (*Blatt/Wurzel*) für As, Cd, Cu, Fe und Mn sowie der TF-Wert (*Stängel/Wurzel*) für Cu größer als 1 sind.

Schlüsselwörter: Sonnenblume, Boden, Schwermetall(oid)e, ICP-OES, Bioakkumulation, Translokation

ISSN 2620-1895